https://doi.org/10.5194/gmd-2021-29
Preprint. Discussion started: 1 March 2021

Geoscientific Model Development Discussions

Sensitivity of different BVOC emission schemes in WRF-Chem(v3.6) to vegetation distributions and its impacts over East China

[1]Mingshuai Zhang, [1,2]Chun Zhao*, [1]Yuhan Yang, [1]Qiuyan Du, [3]Yonglin Shen, [1]Shengfu Lin, [4]Dasa Gu

[1]School of Earth and Space Sciences, University of Science and Technology of China, Hefei, China

[2]CAS Center for Excellence in Comparative Planetology, University of Science and T echnology of China, Hefei, China

[3]School of Geography and Information Engineering, China University of Geosciences, Wuhan 430074, China

[4]Division of Environment and Sustainability, Hong Kong University of Science and Technology, Clear Water Bay, Hong Kong SAR, China

*Corresponding author: Chun Zhao (chunzhao@ustc.edu.cn)

Key points:

1. Modeling performance of BVOC and its impact over East China using different versions (v1.0, v2.0, v3.0) of Model of Emissions of Gases and Aerosols from Nature (MEGAN) in WRF-Chem(v3.6) are examined and documented.
2. Three versions of MEGAN show different sensitivity to vegetation distributions and simulate different seasonal variations of BVOC emissions over East China.
3. Temperature-dependent factor dominates the seasonal change of activity factor in all three versions of MEGAN, while the different response to the change of leaf area index determines the difference among the three versions in seasonal variation of BVOC emissions.
4. The surface ozone concentration can be significantly affected by BVOC emissions over East China, but the impact is sensitive the MEGAN versions.

https://doi.org/10.5194/gmd-2021-29
Preprint. Discussion started: 1 March 2021

Geoscientific Model Development Discussions

Abstract

Biogenic volatile organic compounds (BVOCs) simulated by current air quality and climate models still have large uncertainties, which can influence atmosphere chemistry and secondary pollutant formation over East China. These uncertainties are generally resulted from two sources. One is from different biogenic emission schemes coupled in model, representing for different treatments of physical and chemistry progresses during the emissions of BVOCs. The other is from the biased distribution of vegetation types over a specific region. In this study, the version of WRF-Chem updated by the University of Science and Technology of China (USTC version of WRF-Chem) from the public WRF-Chem(v3.6) is used. The modeling results over East China with different versions (v1.0, v2.0, v3.0) of Model of Emissions of Gases and Aerosols from Nature (MEGAN) in WRF-Chem are examined and documented. Sensitivity experiments with these three versions of MEGAN and two vegetation datasets are conducted to investigate the difference of three MEGAN versions in modeling biogenic VOCs and its dependence on the vegetation distributions. The experiments are also conducted for spring (April) and summer (July) to examine the seasonality of the modeling results. The results indicate that MEGANv3.0 simulates the largest amount of biogenic isoprene emissions over East China. The different performance among MEGAN versions is primarily due to their different treatments of applying emission factors and vegetation types. In particular, the results highlight the importance of considering sub-grid vegetation fraction in estimating BVOCs emissions. Among all activity factors, temperature-dependent factor dominates the seasonal change of activity factor in all three versions of MEGAN, while the different response to the leaf area index (LAI) change determines the difference among the three versions in seasonal variation of BVOC emissions. The simulated surface ozone concentration due to BVOCs can be significantly different among the experiments with three versions of MEGAN, which is mainly due to their impacts on surface VOCs and NOx concentrations. This study suggests that there is still large uncertain range in modeling BVOCs and their impacts on photochemistry and ozone production. More accurate vegetation distribution and measurements of biogenic emission flux and species concentration are needed to evaluate the model performance and reduce the uncertainties.

https://doi.org/10.5194/gmd-2021-29
Preprint. Discussion started: 1 March 2021


Geoscientific Model Development Discussions

1. Introduction

Volatile organic compounds (VOCs) in the atmosphere are from biogenic and anthropogenic sources. Previous studies have indicated that biogenic emission is the dominant source of VOCs, accounting for about 90% of total emissions at global scale (Guenther et al., 1995). Biogenic VOCs (BVOCs) plays a critical role in atmosphere chemistry because some species such as isoprene and monoterpenes are reactive, and can participate in atmospheric photochemical reactions. Therefore, BVOCs could have significant impact on the formation of ozone and secondary organic aerosol (SOA) and ultimately air quality and climate change (Pierce et al., 1998; Carslaw et al., 2000; Poisson et al., 2000; Zhang et al., 2000; Carlton et al., 2009; Brown et al., 2013; Hantson et al., 2017). Among the BVOCs species, isoprene is one of the key identified species that dominates the BVOCs emissions. Global estimation also shows that biogenic isoprene emission is approximately half of total BVOCs emissions (Guenther et al., 2012).

Due to the importance of BVOCs for atmospheric environment, progress has been made extensively in modeling BVOCs emission and its impacts regionally and globally over the past several decades (Geron et al., 1994; Guenther et al., 1995; Niinemets et al., 1999; Arneth et al., 2007). BVOCs emissions are normally estimated with numerical schemes, such as the Seasonal Isoprene synthase Model-Biochemical Isoprenoid biosynthesis Model (SIM-BIM) (Lehning et al., 2001; Zimmer et al., 2003), the Biogenic Emission Inventory System (BEIS)(Pierce et al., 1998), the Global Biosphere Emissions and Interactions System (GloBEIS3) (Yarwwod et al., 2002), the semi-empirical BVOC emission model (seBVOC) (Stewart et al., 2003), and the Model of Emissions of Gases and Aerosols from Nature (MEGAN) (Guenther, 2006; Guenther et al., 2012; Zhao et al., 2016; Jiang et al., 2018). MEGAN is one of the widely used emission schemes for estimating BVOCs emissions under different environmental conditions, and has been coupled with multiple chemical transport models to include the contributions of BVOCs to the variations of air pollutants (Levis et al., 2003; Yang et al., 2011; Ghude et al., 2013; Situ et al., 2013; Tie et al., 2013; Li and Xie, 2014;

https://doi.org/10.5194/gmd-2021-29
Preprint. Discussion started: 1 March 2021


Geoscientific Model Development Discussions
Open Access
EGU

Forkel et al., 2015; Kota et al., 2015; Liu et al., 2018; Wu et al., 2020). However, there still remain larger uncertainties in the estimation of BVOCs emission with MEGAN, due to the uncertain emission rates of some compounds, the limited knowledge of environmental activity factors controlling the BVOCs emissions, the accuracy of vegetation distributions, and etc. (Guenther, 2013).

WRF-Chem (Weather Research and Forecasting model coupled with Chemistry) is an online coupled meteorology and chemistry model that can simulate meteorology fields and chemical species simultaneously (Grell et al., 2005; Fast et al., 2006). The MEGAN scheme is widely used for estimating biogenic emissions online with WRF-Chem (Jiang et al., 2012a; Wang et al., 2015; Abdi-Oskouei et al., 2018; Wei et al., 2018; Arghavani et al., 2019; Safronov et al., 2019; Visser et al., 2019; Li et al., 2020; Yin et al., 2020). The public versions (v4.2 and older) of WRF-Chem include the first MEGAN version (referred to as MEGANv1.0 hereafter) (Guenther et al., 1995) and the second version (referred to as MEGANv2.0 hereafter) (Guenther, 2006). The first version is an earlier scheme with simple canopy treatment and chemical mechanism, considering only the environmental effects from light and temperature on emission flux, and therefore is mainly used in previous studies (e.g., (Guenther et al., 1996; Derognat et al., 2003) but not often in recent studies. Comparatively, MEGANv2.0 is more commonly used for calculating the BVOC emissions with WRF-Chem recently (Geng et al., 2011; Jiang et al., 2012b; Zhang et al., 2015; Zhou et al., 2017) due to its treatment of additional chemical compounds and plant types for emissions. It also considers more complex environmental controlling processes. MEGANv2.1 (Guenther et al., 2012) was recently coupled with WRF-Chem embedded in the CLM4 land surface scheme (Zhao et al., 2016), so that MEGAN obtains the meteorological fields that are calculated online and the consistent vegetation types from the land surface scheme. Although all these three MEGAN versions were coupled in WRF-Chem and used for estimating BVOCs emissions, so far the difference among these MEGAN versions in terms of modeling BVOCs emission and its impacts in WRF-Chem is not examined and documented.

With the rapid increase in economic development during the past several decades,

https://doi.org/10.5194/gmd-2021-29
Preprint. Discussion started: 1 March 2021


Geoscientific Model Development Discussions

East China has become the most prosperous and developed region of China's economy. More and more air pollutants and precursors are emitted into the atmosphere over the region. Previous studies have found that BVOCs play important roles on air pollutant production over East China (e.g., (Han et al., 2005; Wei et al., 2007; Wang et al., 2008; Fu et al., 2010; Zheng et al., 2010; Li et al., 2015a; Li et al., 2015b). Tie et al. (2013) found that the ozone formation was strongly VOC-limited in Shanghai of East China and its production could partly attributed to the biogenic emission of isoprene. Jiang et al. (2012b) investigated the impacts of local biogenic and anthropogenic emissions to the daytime mean ozone mixing ratios over East China using WRF-Chem with MEGANv2.0. Geng et al. (2011) applied WRF-Chem with MEGANv2.0 for studying the effect of isoprene on ozone formation in Shanghai, and they found that the BVOCs from the major forest surrounded have significant impact on ozone production through two different mechanisms. Li et al. (2017a) employed WRF-Chem with MEGANv2.0 to estimate the relative contribution of biogenic and anthropogenic sources to ozone concentration over East China, and concluded that the BVOCs contributed significantly to the background ozone concentration. Wang et al. (2019) founded that the ozone concentration in south of Shanghai can be enhanced significantly due to the mixing of the emissions of BVOCs from the forest and precursors from the ships.

Since the WRF-Chem model with different MEGAN versions has been widely used for studying the impacts of BVOCs on air quality over East China while the performance of different MEGAN versions in WRF-Chem has not been examined, this study aims to investigated the difference of MEGAN versions in terms of modeling BVOCs, focusing on biogenic isoprene, and its impact on ozone concentration over East China. This study updates the MEGANv2.1 coupled by Zhao et al. (2016) to the latest version MEGANv3.0 (see details in Section 2.2), and analyzes the difference of WRF-Chem modeling results with MEGANv1.0, MEGANv2.0, and MEGANv3.0. Numerical experiments are conducted for April and July of 2015 to reflect the seasonal variation of biogenic isoprene emissions and its potential impacts. In order to examine the different sensitivities of MEGAN versions in WRF-Chem to vegetation distributions, two land-use datasets are adopted in this study, which are USGS24

https://doi.org/10.5194/gmd-2021-29
Preprint. Discussion started: 1 March 2021


Geoscientific Model Development Discussions

(United States Geological Survey 24 categories classification) and MODIS2015 (a new dataset derived from the satellite retrievals in this study representing the land-use condition of 2015). The paper is organized as following. Section 2 describes the numerical experiments and methods. The results and discussions are presented in Section 3. A summary is provided in Section 4.

2. Methodology

2.1.WRF-Chem

The version of WRF-Chem updated by University of Science and Technology of China (USTC version of WRF-Chem) is used in this study. Compared with the publicly released version, this USTC version of WRF-Chem includes some additional functions such as the MEGAN scheme implemented in the land surface model (Zhao et al., 2013a; Zhao et al., 2013b; Zhao et al., 2014; Zhao et al., 2016). The configuration of WRF-Chem in this study is similar to that used by (Zhao et al., 2016). In brief, the CBM-Z photochemical mechanism (Zaveri and Peters, 1999) is selected to simulate the gas-phase chemistry that contains 55 prognostic species and 134 reactions. The photolysis rates is computed by the Fast-J radiation parameterization (Wild et al., 2000), and the Yonsei University (YSU) scheme (Hong et al., 2006) is for planetary boundary layer (PBL) parameterization. All of the WRF-Chem simulations use the Morrison two-moment scheme (Morrison et al., 2009) for cloud physics, the Monin–Obukhov similarity theory (Paulson, 1970) for surface layer, the Kain–Fritsch scheme (Kain, 2004) to simulate sub-grid scale clouds and precipitation and the rapid radiative transfer parameterization (RRTMG) for both longwave and shortwave radiation (Iacono et al., 2008).

2.2 MEGAN implemented in WRF-Chem

MEGAN is a widely used scheme for calculating biogenic emissions from terrestrial system to atmosphere with the impact from different environmental conditions, such as radiation, temperature, soil moisture, and leaf area. Three versions of MEGAN online coupled with WRF-Chem are used in this study, MEGANv1.0,

https://doi.org/10.5194/gmd-2021-29
Preprint. Discussion started: 1 March 2021


Geoscientific Model Development Discussions

MEGANv2.0, and MEGANv3.0 that is updated from MEGANv2.1 as implemented by (Zhao et al., 2016) according to the changes made by Jiang et al. (2018) and the technical description of CLM4.0 (Oleson et al., 2010).

MEGAN in WRF-Chem estimates biogenic emission (F_i) of different chemical compounds (i) based on emission factors (ε_i) (μg m^{-2} h^{-1}), activity factors (γ_i) that is controlled by environmental conditions, and the lost and production rate within the plant canopy (ρ).

$$F_i = \varepsilon_i \times \gamma_i \times \rho \quad (1)$$

Where ε_i is a PFT weighted value that is calculated by PFT specific emission factor $\varepsilon_{i,j}$ and grid box area coverage fraction $f_{PFT(j)}$ of PFT(j), i.e., $\varepsilon_i = \sum \varepsilon_{i,j} f_{PFT(j)}$ and γ_i is the product of each activity factor such as leaf-level photosynthetic photon flux density (PPFD)(γ_P), temperature(γ_t), leaf area index (LAI) (γ_{LAI}) and leaf age(γ_a), i.e.,$\gamma_i = \gamma_{LAI}\gamma_P\gamma_t\gamma_a$

MEGANv1.0 is the first model version coupled in WRF-Chem. It considers only the response of emission to radiation and temperature. The mechanism of environmental impact is very simple compared with the later versions. For emission factors, MEGANv1.0 follows the land surface scheme with 24 land use types and prescribes emission factor for each land-use type (Fig. 2). It groups the 24 land-use types into the 6 plant categories (urban or bare soil, agriculture, grassland, deciduous forest, mixed forest, and other natural land) for calculating biogenic emission activity factor.

Guenther (2006) introduced MEGANv2.0 that is a major update from the previous version. In the version of WRF-Chem used in this study, it is separated to estimate emission factor at each grid cell for isoprene and other BVOCs, respectively, although the public offline MEGANv2.0 has the option to calculate isoprene emission factor based on PFT. In WRF-Chem, the emission factor is prescribed for isoprene emission at each grid cell, and calculated for other BVOCs using PFT-specified emission factors and PFT cover database. The vegetation distributions can also be customized. For activity factor, the impacts of PPFD, temperature, monthly LAI, leaf age, soil moisture,

https://doi.org/10.5194/gmd-2021-29
Preprint. Discussion started: 1 March 2021


Geoscientific Model Development Discussions

and solar radiation on biogenic emissions are taken into account (Guenther, 2006). However, there are some shortcomings in MEGANv2.0 implemented in public version of WRF-Chem. MEGANv2.0 uses the monthly mean surface air temperature, LAI and solar radiation from the climatological database that may not be consistent with the meteorological fields during the simulation. In addition, the vegetation distribution at each grid cell used in MEGANv2.0 (only 4 dominant PFT) is prescribed as different from the one used in the land surface scheme (e.g., 24 land use types). Zhao et al. (2016) implemented MEGANv2.1 into CLM4.0 in WRF-Chem so that the biogenic emission scheme and the land surface scheme can use the consistent distributions of vegetation type, surface air temperature, LAI and solar radiation. For emission factors, MEGANv2.1 defines as the net primary emission that escaped into the atmosphere and it does not contain the downward flux of chemicals from above canopy, while MEGAN 2.0 defines as the total flux of chemical compounds, detailed in Zhao et al. (2016).

Recently, Jiang et al. (2018) established the relationship between photosynthesis and water stress and the BVOCs emissions that is not included in MEGANv2.1 in WRF-Chem. They presented a more sophisticated mechanistic representation of BVOCs emission in MEGAN (referred to as MEGANv3.0 hereafter) to simulate the impact of drought on biogenic isoprene emissions. Following Jiang et al. (2018), the MEGANv2.1 in WRF-Chem is updated to MEGANv3.0 in this study to include the effect of drought on biogenic emissions, in which the new drought activity factor $\gamma_{d,isoprene}$ is calculated as the following formula:

$$\gamma_{d,isoprene} = 1 \qquad (\beta_t > 0.6)$$
$$\gamma_{d,isoprene} = V_{cmax}/\alpha \qquad (\beta_t < 0.6, \alpha = 37) \tag{2}$$

where α is an empirical and regionally applicable value derived from field measurements at observation site in Missouri Ozarks AmeriFlux site (MOFLUX) to limit and modify the isoprene emission due to the drought force. Therefore, the value of α may not be suitable for China. However, due to the lack of observations in China, the default α value is used in this study. V_{cmax} is the photosynthetic enzyme activity, and β_t is the soil water stress function calculated as following:

$$\beta_t = \sum w_i r_i \tag{3}$$

https://doi.org/10.5194/gmd-2021-29
Preprint. Discussion started: 1 March 2021


Geoscientific Model Development Discussions
Open Access
EGU

where w_i is the wilting factor based on soil water potential at each soil layer, and r_i is the fraction of roots in soil layer. More details can be found in the CLM4.0 technical notes (Oleson et al., 2010).

2.3 Vegetation distribution

Zhao et al. (2016) suggested that the distributions of vegetation types play an important role in determining regional emissions of BVOCs with MEGAN. Two vegetation datasets are used to examine the sensitivities of BVOCs emissions with different MEGAN versions to vegetation distributions. One is the default land cover dataset (USGS24) used in WRF-Chem (referred to as VEG-USGS hereafter), which generally represents the land cover information for 1990s over East China (Loveland et al., 2000). It is converted to 16-PFT data set in CLM4.0 (referred to as VEG-USGS hereafter) following the table derived by Bonan (1996) as Zhao et al. (2016). Specific descriptions of legend and class of the land cover data are listed in the Table 1. Another land cover dataset is derived from the MODIS retrievals in 2015 (referred to as VEG-2015 hereafter), which has the horizontal resolution of 1 km over entire China. VEG-2015 were reclassified on the existing products of 2015, including GFSAD1000 (Cropland Extent 1km Crop Dominance, Global Food-Support Analysis Data) (Thenkabail et al., 2012), and MODIS MCD12Q1 (MODIS Land Cover Type Yearly Global 500m) product (Friedl et al., 2002). For MCD12Q1 product, there are six different classification schemes (Gregorio, 2005), in which the two schemes of FAO (Food and Agriculture Organization) LCCS (Land Cover Classification System) land cover and FAO LCCS surface hydrology were used.

Figure 1 shows the spatial distributions of the dominant PFT within each model grid cell (see details in Section 2.4) over East China from these two vegetation datasets. It is apparent that VEG-2015 is much different from VEG-USGS. The Z-shaped urban belt of Yangtze River Delta region is evident in VEG-2015 but not in VEG-USGS. Not only the dominant PFT but also the sub-grid distributions of PFTs are different between the two datasets (not shown). Table 1 illustrates the percentage of each PFT averaged over the simulated domain from the two vegetation data sets. For example, the fraction

https://doi.org/10.5194/gmd-2021-29
Preprint. Discussion started: 1 March 2021


Geoscientific Model Development Discussions

of needleleaf evergreen tree that is a major species of biogenic emission range from 7.9% in VEG-USGS to 1.7% in VEG-2015, and the fraction of bare soil is nearly twice that of VEG-USGS. The emissions of BVOCs from MEGAN could be significantly different due to this difference. The sensitivity of MEGAN estimated BVOCs emission to different vegetation distributions may also be different for different versions.

2.4 Numerical experiments

In this study, the simulations are conducted with a horizontal resolution of 12km and 120×100 grid cells (109.3°E~125.6°E,25.4°N~36.4°N) over East China. The simulation periods are April and July of 2015 representing one month of spring and summer, respectively, to reflect the seasonal variation of biogenic emission. The quasi-global WRF-Chem simulation with 360×145 grid cells (180°W~180°E,67.5°S~77.5°N) at the 1°×1° horizontal resolution is used to provide the chemical boundary condition. The meteorological initial and lateral boundary conditions are obtained from the NCEP Final reanalysis data with 1°×1° resolution and updated every 6 hours. The modeled u and v component wind and temperature in atmosphere above the planetary boundary layer are nudged towards the NCEP Final reanalysis data with a 6-hour timescale (Stauffer and Seaman, 1990).

Anthropogenic emissions for these simulations are obtained from the Hemispheric Transport of Air Pollution verison-2 (HTAPv2) at 0.1°×0.1° horizontal resolution and monthly temporal resolution for 2010 (Janssens-Maenhout et al., 2015), while the Multi-resolutions Emission Inventory for China (MEIC) at 0.1°×0.1° horizontal resolution for 2015 (Li et al., 2017b; Li et al., 2017c) is used to replace the emissions over China within the simulation domain. Biomass burning emissions are obtained from the Fire Inventory from NCAR (FINN) at 1 km horizontal resolution and hourly temporal resolution (Wiedinmyer et al., 2011) and follow the injection heights proposed by Dentener et al. (2006) in the Aerosol Comparison between Observations and Models (AeroCom) and the diurnal variation provided by WRAP (2005). The GOCART dust emission scheme (Ginoux et al., 2001) is used to calculated the vertical dust flux, and

https://doi.org/10.5194/gmd-2021-29
Preprint. Discussion started: 1 March 2021


Geoscientific Model Development Discussions

the dust particles emitted into atmosphere are distributed by the MOSAIC aerosol size bins based on the physics of scale-invariant fragmentation of brittle materials provided by Kok (2011) . Sea-salt emissions is similar to Zhao et al. (2013a), which corrected particles with radius less than 0.2 μm and considered the dependence of the temperature of sea surface. More detailed about the sea-salt emissions and dust emission scheme coupled with MOSAIC aerosol scheme in WRF-Chem can be found in (Zhao et al., 2010)).

In order to investigate the sensitivities of simulated biogenic isoprene emissions by different versions of MEGAN to different vegetation distributions, as mentioned above, multiple experiments are conducted with different vegetation datasets and MEGAN versions, as summarized in Table 2. First of all, three experiments are conducted with the USGS vegetation distribution (VEG-USGS) using different versions of MEGAN embedded in WRF-Chem as discussed above, i.e., MEGANv1.0 (Mv1-USGS), MEGANv2.0 (Mv2-USGS), and MEGANv3.0 (Mv3-USGS). The sensitivities of biogenic emissions to different versions of MEGAN can be explored by comparing these three experiments. Second, another three experiments are conducted similar to the former ones but the VEG-USGS dataset is replaced by the VEG-2015 dataset, i.e., Mv1-2015, Mv2-2015, and Mv3-2015, respectively. By comparing these two sets of experiments, the impacts of the two vegetation distributions on the simulated BVOC emissions with each version of MEGAN can be investigated. These six experiments are conducted for both April and July. The seasonal variation of the sensitivities of BVOC emissions to different MEGAN versions and vegetation distributions can be explored through the simulations for these two months.

3. Results

3.1 Biogenic isoprene emission

3.1.1 Sensitivity to emission schemes and vegetation distributions

Figure 3 shows the spatial distributions of biogenic isoprene emission averaged in April for six simulations with different vegetation datasets and biogenic emission

https://doi.org/10.5194/gmd-2021-29
Preprint. Discussion started: 1 March 2021


Geoscientific Model Development Discussions

schemes. First of all, with the same vegetation dataset of USGS, the large difference exists among the results from these three versions of emission scheme. In terms of domain average, MEGANv2.0 simulates the highest isoprene emission among the three versions, MEGANv3.0 follows, and MEGANv1.0 simulates the lowest, especially over the northwest of the simulation domain. It can also be noticed that the spatial distributions of biogenic isoprene emission are different among the versions. To illustrate better the difference, two focused areas (denoted by the red and black boxes in Fig. 3) in the simulation domain are selected for further analysis. Over the southwest region of domain (denoted by the black box), the averaged biogenic isoprene emission in Mv1-USGS is below 0.2 mole/km^2/hr, and it is about 1.0 mole/ km^2/hr and 3.1 mole/km^2/hr from the Mv3-USGS and Mv2-USGS simulations, respectively. Over the southeast region of domain (denoted by the red box), similarly, the MEGANv2.0 simulates the highest biogenic isoprene emission among the three versions and MEGAN v1.0 estimates more emissions than MEGAN v3.0.

Over the southwest region of domain, for MEGAN v1.0, irrigated cropland (the 3rd land use type in VEG-USGS), cropland with grassland mosaic (the 5th), and savanna (the 10th) are the dominant land use types over the southwest region (Fig. 1), which have low emission factors (as shown in Fig. 2). For MEGAN v3.0, crop and grass are the dominant PFTs over the region, but some temperate needle-leaf evergreen trees that have higher emission factor of about 3 mg isoprene/m^2/hr (as shown in Fig. 3) are also included in this area (Fig. 1). The different vegetation distributions lead to the overall emission factors are different between MEGANv1.0 and MEGANv2.0 (Fig. 4). Therefore, MEGAN v3.0 simulated more biogenic isoprene emissions than MEGAN v1.0 (0.88 mole/km^2/hr versus 0.42 mole/km^2/hr) over this region. Over the southeast region of domain, the dominant land use type is cropland with woodland mosaic (the 6th) that has high emission factor of about 2 mg isoprene/m^2/hr and irrigated cropland in MEGAN v1.0. By contrast, the PFTs in MEGAN v3.0 is crop and has lower emission factor. This leads to larger overall emission factor in MEGANv1.0 than in MEGANv3.0 over this region. Therefore, MEGANv1.0 calculates more biogenic isoprene emissions than MEGANv3.0 (1.08 mole/km^2/hr versus 0.65 mole/km^2/hr) over the area. In

https://doi.org/10.5194/gmd-2021-29
Preprint. Discussion started: 1 March 2021


Geoscientific Model Development Discussions

general, the difference between MEGANv1.0 and MEGANv3.0 with the same USGS land-use dataset is mainly due to the conversion of the USGS land-use to PFT that leads to different vegetation types with different emission factors in each grid. For MEGANv2.0, the emission factor of isoprene is obtained from the input database directly in WRF-Chem, and it is the highest among the three versions of MEGAN (Fig. 4). Therefore, MEGANv2.0 simulates the most biogenic isoprene emissions over the two analyzed regions among the three different versions independent of the vegetation coverage (will be discussed below).

In terms of the modeling sensitivities to vegetation distributions (i.e., VEG-USGS versus VEG-2015), as discussed above, with prescribed emission factor of isoprene at each grid cell, the isoprene emission from MEGANv2.0 in WRF-Chem does not change much with different vegetation distributions except some small perturbation due to the impacts of vegetation distributions on meteorological fields. Over the southwest of domain, the averaged biogenic isoprene emission with VEG-2015 is higher (0.68 mole/km^2/hr and 2.25 mole/km^2/hr) than that (0.42 mole/km^2/hr and 0.88 mole/km^2/hr) with VEG-USGS for both MEGANv1.0 and MEGANv3.0 due to the increased fraction of needle-leaf evergreen tree and mixed forest over this area (Fig. 1) in VEG-2015, and these land use types have higher emission factors (Fig. 2) than croplands in VEG-USGS. Over the southeast, the vegetation coverage is significantly reduced from VEG-2015 to VEG-USGS due to the rapid development in economic and unban expansion over the region in last two decades. Therefore, for MEGANv1.0, the averaged isoprene emission from Mv1-2015 is lower (0.39 mole/km^2/hr) than that (1.08 mole/km^2/hr) from Mv1-USGS, consistent with the lower overall emission factor with VEG-2015 compared to VEG-USGS in MEGANv1.0 (Fig. 4). However, it is noteworthy that, for MEGANv3.0, the isoprene emission from Mv3-2015 is higher (1.12 mole/km^2/hr) than that (0.65 mole/km^2/hr) from Mv3-USGS. The different sensitivities of the two versions to the vegetation changes are mainly due to their different treatments of sub-grid vegetation distribution as discussed in Sect. 2.2, i.e., MEGANv3.0 considers sub-grid vegetation distribution besides the dominant vegetation type at each grid cell when estimate the BVOCs emissions, while

https://doi.org/10.5194/gmd-2021-29
Preprint. Discussion started: 1 March 2021

MEGANv1.0 only considers the dominant vegetation type at each grid cell.

To further demonstrate the impact of sub-grid distribution of vegetation in MEGANv3.0, Figure 5 shows the difference of major sub-grid fraction of PFT other than the dominant one over the southeast region of domain within the red box between VEG-2015 and VEG-USGS. Although the dominant vegetation types are crops, grass, and bare soil over the region (Fig. 1), the sub-grid fractions of needle-leaf evergreen tree, broad-leaf evergreen tree, and broad-leaf deciduous tree that have relatively higher emission factors (Fig. 2) are higher in VEG-2015 than in VEG-USGS. As shown in Fig. 4, the overall emission factor $\varepsilon_{i,j}$ weighted by sub-grid PFT fractions is higher with VEG-2015 than with VEG-USGS from MEGANv3.0. It highlights that the sub-grid vegetation distribution is important in terms of estimating BVOC emissions over this region, which results in more biogenic isoprene emission in MEGANv3.0 than MEGANv1.0 with the latest vegetation distribution dataset (i.e., VEG-2015).

3.1.2 Environmental impacts

Besides emission factor, biogenic emission is also influenced by activity factor that is largely controlled by environmental conditions. The activity factor mainly accounts for the response of biogenic emission to temperature, leaf age, soil moisture, solar radiation, leaf area index, and drought in current versions of MEGAN. The seasonal variations (July versus April) of simulated biogenic emissions by different versions of MEGAN with VEG-2015 are investigated to demonstrate the environmental impacts and their difference among MEGAN versions. Please note that emission factors are not dependent on seasons. Figure 6 shows the ratios of monthly averaged biogenic isoprene emission and overall activity factor (γ_i) between July and April from three versions of MEGAN with the VEG-2015 vegetation dataset. Only the simulation results with VEG-2015 are analyzed here due to the similar results with VEG-USGS (not shown). It is evident that the ratios are all greater than one, which means much more isoprene is emitted into atmosphere by plant in July than in April. The seasonal variations of magnitudes and the distributions of activity factors are consistent with those of emissions. Among different versions, MEGANv3.0 is most sensitive to

https://doi.org/10.5194/gmd-2021-29
Preprint. Discussion started: 1 March 2021


Geoscientific Model Development Discussions

environmental conditions, especially over the north of domain between 32°N and 36°N.

The overall activity factor is the product of the factors determined by temperature, LAI, solar radiation, leaf age, and drought condition in MEGANv2.0 and MEGANv3.0 while it is an overall function of temperature and solar radiation in MEGANv1.0 that cannot be separated as isolated factors. Therefore, for MEGAN v2.0 and MEGAN v3.0, the ratios of isolated activity factors responding to temperature, LAI, solar radiation, leaf age, and drought between July and April are further illustrated in Figure 7. The temperature-dependent activity factor (γ_t) plays an important role in the seasonal change of total activity factor, especially in the north of simulation domain, which is about 3.0~4.0 and >4.0 in MEGANv2.0 and MEGANv3.0, respectively, which means that MEGAN predicts higher biogenic isoprene emission in warmer environment. Guenther (2006) also point that the temperature-dependent activity factor increases evidently with temperature.

There are two activity factors associated with leaves. One is related to the emission dependence of absolute values of LAI (γ_{LAI}), which has the most different distributions among all activity factors in two versions. The ratio in MEGAN v3.0 is above 4 and < 2 in MEGAN v2.0 over the most part of simulation domain. It is noteworthy that the ratio is below 1 in MEGAN v2.0 in the north of the domain while it is more than 4 in MEGAN v3.0, that dominant the difference between July and April. Figure 8 shows the change of activity factor for LAI as a function of LAI value used in MEGAN v2.0 and MEGAN v3.0, respectively. It is evident that the estimated LAI activity factors in both versions increase with the LAI values, but with different increasing rates. In general, MEGANv3.0 has the faster increasing rate. Please note, as discussed previously in Sect. 2.2, MEGAN v3.0 obtains the LAI online from the land surface scheme directly that can capture the seasonal change well, while MEGAN v2.0 obtains it from climatological monthly mean input dataset that is different from the one used in the land surface scheme in WRF-Chem. Figure 9 shows the distributions of LAI in MEGAN v2.0 and MEGAN v3.0 in different months. For MEGAN v2.0, LAI has almost no change from April to July, particularly over the northern simulation domain, while for MEGAN v3.0, the LAI increases evidently over the whole domain, especially

https://doi.org/10.5194/gmd-2021-29
Preprint. Discussion started: 1 March 2021


Geoscientific Model Development Discussions

over the north. Therefore, the ratio of γ_{LAI} between July and April is around one in MEGANv2.0, while it is much larger than one in MEGANv3.0.

The second is related to the leaf age (γ_a) that also has quite different distributions between MEGANv2.0 and MEGANv3.0. For MEGAN v2.0, the ratio is about 1~3 in the most area while it below 1.0 between 30°N and 34°N, and more than 2 in the northwest of simulation domain. For MEGAN v3.0, the ratio is above 1.0 over the whole domain and the distribution has significant regional difference. It is 1~1.3 in the south region while more than 2 in the north region. Generally speaking, leaf's ability to emit biogenic isoprene is significantly influenced by leaf phenology. Young leaves emit almost no isoprene, mature leaves emit mostly, and old leaves lose ability to produce biogenic isoprene eventually. Therefore, plants emit more isoprene into atmosphere in July than in April because of more mature leaves due to the plant growth. Activity factor for leaf age is a function of the relative change of emission activity and the fraction of leaves at different phenological stages that are determined by the difference of LAI in current and previous month. In both versions of MEGAN, mature and old foliage have highest relative isoprene emission activity, following by the growing foliage and the new foliage is the lowest. Therefore, MEGAN v3.0 produce higher leaf age activity factor in July because of the larger difference of LAI in different month and more mature foliage to emit isoprene (Fig. 9).

The distribution of the ratio of light-depend activity factor (γ_P) is also different between the two versions. Light-depend activity factor (γ_P) is a function of PPFD and activity of isoprene synthase, and is dominated by the variation of PPFD. In general, plants often have higher light-depend activity factor in July than that in April due to the stronger radiation. For MEGAN v2.0, it is about 1~1.5 over the whole domain and has no significant regional difference. For MEGAN v3.0, the ratio is below 1 in the south of the domain while it is about 1.3~1.5 or more than 2 in the north of the domain. MEGAN v3.0 considered the difference of sunlit and shaded leaves and PPFD will be low on shaded leaves in dense canopy because of the blocking sunlight. Therefore, MEGAN v3.0 calculated low light-depend activity factor in the south of the domain due to the distribution of mixed forest which has dense canopy in summer.

https://doi.org/10.5194/gmd-2021-29
Preprint. Discussion started: 1 March 2021

The seasonal variation of drought-dependent activity factor ($\gamma_{d,isoprene}$) is only included in MEGANv3.0 with the ratios of 1~3 over the domain. Previous studies have shown that plants emit more isoprene into atmosphere under short-term mild drought stress (e.g., Jiang et al., 2018). The reduction of stomatal conductance is accompanied with the increase in leaf temperature resulting in the more isoprene emissions from plants (Jiang et al., 2018). In addition, as discussed in the Section 2.2, drought-dependent activity factor is proportional to photosynthetic enzyme activity, which can be affected by PPFD. Therefore, MEGAN v3.0 estimated more isoprene emissions in July especially in the north of domain and the pattern is similar to the distribution of light-depend activity factor.

3.1.3 Comparison with observations

The results discussed above show the difference in modeling biogenic emissions of isoprene. The difference of simulated near-surface isoprene concentrations is similar as their emissions (not shown here). It will be optimal to compare the simulated isoprene emissions and concentrations from different experiments with observations. However, as far as we know, the publicly available in-situ measurements of isoprene emissions and concentrations over East China is extremely sparse. Meanwhile, although the satellite retrieved column integrated formaldehyde is often used for evaluating simulated BVOCs, it is not suitable for using in this study because the production from anthropogenic VOCs dominates the column formaldehyde over most regions of East China. It is difficult to isolate the contribution from BVOCs to formaldehyde from satellite retrievals. Since it is difficult to evaluate the simulated results over a large area of East China, the limited observations are collected from published literatures and unpublished data over both rural and urban areas of East China to compare with the results of different experiments as listed in Table 3.

In general, the simulated results with MEGANv2.0 and MEGANv3.0 are closer to measurements. MEGANv1.0 generally underestimates the observed values. Although the results from MEGANv2.0 and MEGANv3.0 are quite different in some cases, they are both within the uncertain range of observations in general. Although, as discussed

https://doi.org/10.5194/gmd-2021-29
Preprint. Discussion started: 1 March 2021


Geoscientific Model Development Discussions

above, MEGANv3.0 can capture the biogenic isoprene emissions in urban area due to its consideration of sub-grid vegetation distributions, it is difficult to be evaluated with these limited data, except that at one site of Shanghai, the simulation with MEGANv3.0 produces higher surface concentration of isoprene that is closer to the observation compared to that with MEGANv2.0. Overall, the experiments with MEGANv2.0 and MEGANv3.0 may simulate better surface concentration of isoprene over East China than that with MEGANv1.0, and more high-quality observations of BVOCs concentrations in both rural and urban areas of East China are definitely needed to further validate the modeling results in future.

3.2 Impacts on mixing ratio of VOCs and ozone

Difference in emissions of BVOCs from multiple versions of MEGAN can influence the simulated mixing ratio of VOCs over East China that can further significantly affect ozone production through photochemistry (Wei et al., 2007; Bao et al., 2010; Calfapietra et al., 2013; Kim et al., 2013; Liu et al., 2018; Lu et al., 2019). The photochemistry is most active in summer, therefore, the simulation results in July with the latest vegetation coverage (VEG-2015) are analyzed here. Figure 10 shows the distributions of total VOCs and HCHO concentrations near the surface contributed by the BVOCs emissions simulated by the model with different versions of MEGAN using VEG-2015 in July. It is evident that BVOCs contribute significantly to the amount of total VOCs over East China, and the difference among the simulations with the three versions of MEGAN is large. The simulation with MEGANv3.0 produces the highest biogenic VOCs concentration (> 20 ppb), followed by MEGANv2.0 (10-20 ppb), and the one with MEGAN v1.0 is the lowest (< 5 ppb), particularly over the northern region. In terms of spatial distribution, the simulation with MEGANv3.0 generates higher biogenic VOCs concentration over the north of domain, while the ones with the other two versions of MEGAN generate higher concentration over the south, which is consistent with the spatial distributions of the total biogenic emissions simulated by different MEGAN versions in WRF-Chem (Fig. S1 in the supporting material). The spatial distributions of simulated biogenic contribution to the surface formaldehyde

https://doi.org/10.5194/gmd-2021-29
Preprint. Discussion started: 1 March 2021


Geoscientific Model Development Discussions

546 concentration are consistent with those of biogenic VOCs.

547 The significantly increased amounts of biogenic VOCs may induce the increase of
548 surface ozone concentration over East China (Zhao et al., 2009). Figure 11
549 demonstrates the spatial distribution of monthly mean ozone mixing ratio near the
550 surface contributed by the emissions of BVOCs. The simulation with MEGANv3.0
551 produces the largest amount of biogenic ozone over a large area of the simulation
552 domain. The biogenic ozone from the simulation with MEGANv3.0 is estimated over
553 8 ppb while it is 2~5 ppb from the one with MEGAN v2.0 and less than 1 ppb from the
554 one with MEGANv1.0. For MEGANv1.0 and MEGAN v3.0, the distributions of
555 surface biogenic ozone concentration is consistent with those of biogenic VOCs, for
556 example, MEGAN v3.0 estimated more biogenic VOCs over the north of the domain
557 while ozone concentration is also simulated higher in the same region. For MEGAN
558 v2.0, it is evident that the ozone formation is not influenced by biogenic VOCs solely.
559 The ozone production can be determined by the changes of both VOCs and NOx
560 concentrations, and the production efficiency can be different for NO_x-sensitive region
561 and VOCs-sensitive region (e.g., Zhao et al., 2009).

562 Figure 12 shows the surface concentrations of NO_x due to the biogenic emissions
563 simulated with three versions of MEGAN with VEG-2015. The results are calculated
564 as the difference between simulations with and without biogenic emissions. The
565 simulations with MEGANv3.0 estimate the highest BVOCS-contributed concentration
566 change, especially over the north of domain (>2 ppb), followed by MEGAN v2.0 (0.2-
567 0.4ppb), and MEGAN v1.0 simulated lowest concentration (about 0.1ppb and below 0).
568 The different changes of surface NOx concentrations are mainly caused by the different
569 impacts on NOx lifetime due to biogenic VOCs. The increase of surface NOx
570 concentration is due to the BVOC-induced increase of NOx lifetime reflected by the
571 reduction of surface OH concentration (Fig. S2 in the supporting material). Therefore,
572 the increase of ozone contributed by biogenic emissions in the north of the domain
573 (30°N-36°N) simulated with MEGANv2.0 is due to the combined effect of increased
574 NO_x and VOCs surface concentrations. It is also noteworthy that the surface ozone
575 concentrations are simulated lower over the southeast of domain than that in the

https://doi.org/10.5194/gmd-2021-29
Preprint. Discussion started: 1 March 2021


Geoscientific Model Development Discussions

576 southwest with the three versions of MEGAN, while the surface concentrations of
577 BVOCs have no significant difference between the two regions. This is mainly due to
578 that the southwest is more sensitive to VOCs in terms of ozone production (Fig. S3 in
579 the supporting material) (e.g., Zhao et al., 2009).
580

581 ## 4. Summary and conclusion

582 In this study, three versions of MEGAN in WRF-Chem and their difference in
583 simulating BVOC emissions and impacts on ozone mixing ratio over East China is
584 documented in the literature for the first time. The latest version of MEGAN v3.0 is
585 coupled within CLM4 land scheme as a part of WRF-Chem. Specifically, MEGAN v3.0
586 is updated from MEGAN v2.1 as an option in biogenic emission schemes and can share
587 the consistent vegetation map and other variables with CLM4 such as surface
588 temperature and leaf area index. What's more, MEGAN v3.0 include the activity factor
589 for drought and the combination of different versions of MEGAN and CLM4 are
590 employed to investigate the sensitivity of the variation of MEGAN versions.
591 Experiments are conducted for April and July over Eastern China with VEG-USGS and
592 VEG-2015 to study the sensitivities of simulated BVOCs by different MEGAN
593 versions in WRF-Chem to seasonal change and the distributions of vegetation. The
594 main conclusions are summarized below.

595 Physical and chemistry processes in these three versions of MEGAN implemented
596 in WRF-Chem are different, and the most intuitive distinction is their different
597 treatments of emission factor of BVOCs. MEGANv1.0 prescribed constant values for
598 different land use categories at each grid cell, and MEGANv2.0 has a stand-alone PFT
599 specific emission factor map. For MEGAN v3.0, the overall emission factor at each
600 grid cell is calculated by PFT-specific emission factor and the fraction of each PFT.
601 Therefore, the biogenic isoprene emissions estimated by three versions of MEGAN are
602 different over the simulation domain. The VEG-USGS and VEG-2015 datasets present
603 quite different distributions of vegetation coverage, which also contributes to the
604 difference of emission factors among different versions. Different versions of MEGAN

https://doi.org/10.5194/gmd-2021-29
Preprint. Discussion started: 1 March 2021


Geoscientific Model Development Discussions

show different sensitivities to the changes of vegetation distributions due to their different treatments of vegetation fraction in estimating emission factors of BVOCs. The results highlight the importance of considering sub-grid vegetation fraction in estimating BVOCs emissions. MEGANv3.0 with sub-grid vegetation distribution simulates higher BVOCs emissions over the urban area of the Yangtze River Delta (YRD) region compared to MEGANv2.0 with only the dominant vegetation type at each grid cell.

Activity factor plays an important role in determining the seasonal change of BVOCs emissions. Simulations with different versions of MEGAN show different seasonal variation of activity factors and thus BVOCs emissions. The results indicated that overall activity factor in July is higher than the one in April in all versions of MEGAN, and MEGAN v3.0 is most sensitive to the seasonal change especially in the north of simulation domain. In general, among all activity factors, temperature-dependent factor dominates the seasonal change of activity factor in all three versions of MEGAN, while the different response to the LAI change determines the difference among the three versions in seasonal variation of BVOC emissions. The additional drought-dependent activity factor in MEGANv3.0 can result in a little higher BVOC emission over East China in July than April due to the increasing photosynthetic enzyme activity, i.e., plants emit more biogenic isoprene in July than that in April under the short-term mild drought forcing. The overall drought impact on BVOC emissions over East China is small as previous studies (e.g., Jiang et al., 2018).

Different BVOCs simulated with the three versions of MEGAN in WRF-Chem lead to the large difference in ozone production. The simulation with MEGANv3.0 produces the highest BVOCs contributed ozone concentration (> 8 ppbv) over East China among the three versions, followed by the simulations with MEGANv2.0 and MEGAN v1.0. The difference of BVOCs contributed ozone among the simulations with three versions of MEGAN is not only affected by the increased concentration of BVOCs but also influenced by the changes of NOx concentration. The simulations with different versions of MEGAN show different distributions of surface NOx concentration due to the BVOCs-induced changes of NOx lifetime. The production

https://doi.org/10.5194/gmd-2021-29
Preprint. Discussion started: 1 March 2021


Geoscientific Model Development Discussions

efficiency of surface ozone concentration over East China due to BVOCs also depends on the regions as NO_x-sensitive or VOCs-sensitive regions.

This study highlights that the simulated emissions of BVOC over East China is sensitive to vegetation coverage, which has also been found by previous studies (e.g., Klinger et al., 2002; Wang et al., 2007). However, this study further demonstrates that the modeling sensitivity to vegetation coverage could be quite different depending on the BVOC emission schemes. Some studies also showed that BVOC emissions can be more than 50% higher in summer than in other seasons (e.g., Li et al., 2020), which may be also sensitive to the formulas of emission activity factors in different emission algorithms as discussed in this study. Large uncertainties in modeling BVOCs emission over East China still exist as reflected by different versions of the scheme, consistent with previous studies that found the off-line calculation with different versions of MEGAN led to significantly different BVOC emissions over China. Although it is evident that surface ozone concentration can be significantly influenced by BVOC emissions over East China through affecting VOCs, OH, and NOx and the BVOC impact is also region-sensitive as found in this and previous works (e.g., Geng et al., 2011; Tie et al., 2013; Liu et al., 2018), this study highlights that the overall impact can be quite sensitive to different algorithms in emission schemes.

Due to these large uncertainties in emission factor, activity factor, and vegetation distribution in estimating BVOC emissions over East China, the observations of BVOC species such isoprene and monoterpene over East China are urgently needed to evaluate the model and then further quantify the impacts of BVOCs on ozone and organic aerosols. In addition, direct measurements of biogenic emission fluxes and/or emission factors and activity factors are needed to constrain different emission algorithm in atmospheric models. Last not the least, the survey of more accurate and higher resolution vegetation distribution based on in-situ investigation and satellite remote sensing should be conducted to support the estimation of BVOC emission over East China.

https://doi.org/10.5194/gmd-2021-29
Preprint. Discussion started: 1 March 2021

Data availability

The released version of WRF-Chem can be downloaded from http://www2.mmm.ucar.edu/wrf/users/download/get_source.html. The updated USTC version of WRF-Chem can be downloaded from http://aemol.ustc.edu.cn/product/list/ or contact chunzhao@ustc.edu.cn. Also, the code modifications will be incorporated the release version of WRF-Chem in future.

Author contributions

Mingshuai Zhang and Chun Zhao designed the experiments, conducted and analyzed the simulations. All authors contributed to the discussion and final version of the paper.

Acknowledgements

This research was supported by the Fundamental Research Funds for the Central Universities, and the National Natural Science Foundation of China (grant 41775146), the USTC Research Funds of the Double First-Class Initiative, and the Strategic Proiority Research Program of Chinese Academy of Sciences (grant XDB41000000). The study used the computing resources from the High-Performance Computing Center of University of Science and Technology of China (USTC) and the TH-2 of National Supercomputer Center in Guangzhou (NSCC-GZ).

https://doi.org/10.5194/gmd-2021-29
Preprint. Discussion started: 1 March 2021

Reference

Abdi-Oskouei, M., Pfister, G., Flocke, F., Sobhani, N., Saide, P., Fried, A., Richter, D., Weibring, P., Walega, J., and Carmichael, G.: Impacts of physical parameterization on prediction of ethane concentrations for oil and gas emissions in WRF-Chem, Atmos. Chem. Phys., 18, 16863-16883, 2018.

Arghavani, S., Malakooti, H., and Bidokhti, A. A.: Numerical evaluation of urban green space scenarios effects on gaseous air pollutants in Tehran Metropolis based on WRF-Chem model, Atmospheric Environment, 214, 116832, 2019.

Arneth, A., Niinemets, Ü., Pressley, S., Bäck, J., Hari, P., Karl, T., Noe, S., Prentice, I. C., Serça, D., Hickler, T., Wolf, A., and Smith, B.: Process-based estimates of terrestrial ecosystem isoprene emissions: incorporating the effects of a direct CO_2-isoprene interaction, Atmos. Chem. Phys., 7, 31-53, 2007.

Bao, H., Shrestha, K. L., Kondo, A., Kaga, A., and Inoue, Y.: Modeling the influence of biogenic volatile organic compound emissions on ozone concentration during summer season in the Kinki region of Japan, Atmospheric Environment, 44, 421-431, 2010.

Bonan, G. B.: Land surface model (LSM version 1.0) for ecological, hydrological, and atmospheric studies: Technical description and user`s guide. Technical note, United States, 1996.

Brown, S. S., Dubé, W. P., Bahreini, R., Middlebrook, A. M., Brock, C. A., Warneke, C., de Gouw, J. A., Washenfelder, R. A., Atlas, E., Peischl, J., Ryerson, T. B., Holloway, J. S., Schwarz, J. P., Spackman, R., Trainer, M., Parrish, D. D., Fehshenfeld, F. C., and Ravishankara, A. R.: Biogenic VOC oxidation and organic aerosol formation in an urban nocturnal boundary layer: aircraft vertical profiles in Houston, TX, Atmos. Chem. Phys., 13, 11317-11337, 2013.

Calfapietra, C., Fares, S., Manes, F., Morani, A., Sgrigna, G., and Loreto, F.: Role of Biogenic Volatile Organic Compounds (BVOC) emitted by urban trees on ozone concentration in cities: A review, Environmental Pollution, 183, 71-80, 2013.

Carlton, A. G., Wiedinmyer, C., and Kroll, J. H.: A review of Secondary Organic Aerosol (SOA) formation from isoprene, Atmos. Chem. Phys., 9, 4987-5005, 2009.

Carslaw, N., Bell, N., Lewis, A. C., McQuaid, J. B., and Pilling, M. J.: A detailed case study of isoprene chemistry during the EASE96 Mace Head campaign, Atmospheric Environment, 34, 2827-2836, 2000.

Dentener, F., Kinne, S., Bond, T., Boucher, O., Cofala, J., Generoso, S., Ginoux, P., Gong, S., Hoelzemann, J. J., Ito, A., Marelli, L., Penner, J. E., Putaud, J. P., Textor, C., Schulz, M., van der Werf, G. R., and Wilson, J.: Emissions of primary aerosol and precursor gases in the years 2000 and 1750 prescribed data-sets for AeroCom, Atmos. Chem. Phys., 6, 4321-4344, 2006.

Derognat, C., Beekmann, M., Baeumle, M., Martin, D., and Schmidt, H.: Effect of biogenic volatile organic compound emissions on tropospheric chemistry during the Atmospheric Pollution Over the Paris Area (ESQUIF) campaign in the Ile-de-France region, J. Geophys. Res.-Atmos., 108, 15, 2003.

Fast, J. D., Gustafson Jr, W. I., Easter, R. C., Zaveri, R. A., Barnard, J. C., Chapman, E.

https://doi.org/10.5194/gmd-2021-29
Preprint. Discussion started: 1 March 2021

G., Grell, G. A., and Peckham, S. E.: Evolution of ozone, particulates, and aerosol direct radiative forcing in the vicinity of Houston using a fully coupled meteorology-chemistry-aerosol model, Journal of Geophysical Research: Atmospheres, 111, 2006.

Forkel, R., Balzarini, A., Baró, R., Bianconi, R., Curci, G., Jiménez-Guerrero, P., Hirtl, M., Honzak, L., Lorenz, C., Im, U., Pérez, J. L., Pirovano, G., San José, R., Tuccella, P., Werhahn, J., and Žabkar, R.: Analysis of the WRF-Chem contributions to AQMEII phase2 with respect to aerosol radiative feedbacks on meteorology and pollutant distributions, Atmospheric Environment, 115, 630-645, 2015.

Friedl, M. A., McIver, D. K., Hodges, J. C. F., Zhang, X. Y., Muchoney, D., Strahler, A. H., Woodcock, C. E., Gopal, S., Schneider, A., Cooper, A., Baccini, A., Gao, F., and Schaaf, C.: Global land cover mapping from MODIS: algorithms and early results, Remote Sensing of Environment, 83, 287-302, 2002.

Fu, P., Kawamura, K., Kanaya, Y., and Wang, Z.: Contributions of biogenic volatile organic compounds to the formation of secondary organic aerosols over Mt. Tai, Central East China, Atmospheric Environment, 44, 4817-4826, 2010.

Geng, F., Tie, X., Guenther, A., Li, G., Cao, J., and Harley, P.: Effect of isoprene emissions from major forests on ozone formation in the city of Shanghai, China, Atmos. Chem. Phys., 11, 10449-10459, 2011.

Geron, C. D., Guenther, A. B., and Pierce, T. E.: An improved model for estimating emissions of volatile organic compounds from forests in the eastern United States, Journal of Geophysical Research: Atmospheres, 99, 12773-12791, 1994.

Ghude, S. D., Pfister, G. G., Jena, C., van der A, R. J., Emmons, L. K., and Kumar, R.: Satellite constraints of nitrogen oxide (NOx) emissions from India based on OMI observations and WRF-Chem simulations, Geophysical Research Letters, 40, 423-428, 2013.

Ginoux, P., Chin, M., Tegen, I., Prospero, J. M., Holben, B., Dubovik, O., and Lin, S.-J.: Sources and distributions of dust aerosols simulated with the GOCART model, Journal of Geophysical Research: Atmospheres, 106, 20255-20273, 2001.

Gregorio, A.: Land Cover Classification System (LCCS), version 2: Classification Concepts and User Manual: LCCS. Number8. Food & Agriculture Organization, Rome, Italy., FAO Environment and Natural Resources Service Series, 8, 2005.

Grell, G. A., Peckham, S. E., Schmitz, R., McKeen, S. A., Frost, G., Skamarock, W. C., and Eder, B.: Fully coupled “online” chemistry within the WRF model, Atmospheric Environment, 39, 6957-6975, 2005.

Guenther, A.: Biological and Chemical Diversity of Biogenic Volatile Organic Emissions into the Atmosphere, ISRN Atmospheric Sciences, 2013, 2013.

Guenther, A.: Estimates of global terrestrial isoprene emissions using MEGAN (Model of Emissions of Gases and Aerosols from Nature), Atmos. Chem. Phys., 7, 4327-4327, 2006.

Guenther, A., Hewitt, C. N., Erickson, D., Fall, R., Geron, C., Graedel, T., Harley, P., Klinger, L., Lerdau, M., Mckay, W. A., Pierce, T., Scholes, B., Steinbrecher, R., Tallamraju, R., Taylor, J., and Zimmerman, P.: A global model of natural volatile

https://doi.org/10.5194/gmd-2021-29
Preprint. Discussion started: 1 March 2021

organic compound emissions, Journal of Geophysical Research: Atmospheres, 100, 8873-8892, 1995.

Guenther, A., Zimmerman, P., Klinger, L., Greenberg, J., Ennis, C., Davis, K., Pollock, W., Westberg, H., Allwine, G., and Geron, C.: Estimates of regional natural volatile organic compound fluxes from enclosure and ambient measurements, J. Geophys. Res.-Atmos., 101, 1345-1359, 1996.

Guenther, A. B., Jiang, X., Heald, C. L., Sakulyanontvittaya, T., Duhl, T., Emmons, L. K., and Wang, X.: The Model of Emissions of Gases and Aerosols from Nature version 2.1 (MEGAN2.1): an extended and updated framework for modeling biogenic emissions, Geoscientific Model Development, 5, 1471-1492, 2012.

Han, Z. W., Ueda, H., and Matsuda, K.: Model study of the impact of biogenic emission on regional ozone and the effectiveness of emission reduction scenarios over eastern China, Tellus Ser. B-Chem. Phys. Meteorol., 57, 12-27, 2005.

Hantson, S., Knorr, W., Schurgers, G., Pugh, T. A. M., and Arneth, A.: Global isoprene and monoterpene emissions under changing climate, vegetation, CO2 and land use, Atmospheric Environment, 155, 35-45, 2017.

Hong, S.-Y., Noh, Y., and Dudhia, J.: A New Vertical Diffusion Package with an Explicit Treatment of Entrainment Processes, Monthly Weather Review, 134, 2318-2341, 2006.

Iacono, M. J., Delamere, J. S., Mlawer, E. J., Shephard, M. W., Clough, S. A., and Collins, W. D.: Radiative forcing by long-lived greenhouse gases: Calculations with the AER radiative transfer models, Journal of Geophysical Research: Atmospheres, 113, 2008.

Janssens-Maenhout, G., Crippa, M., Guizzardi, D., Dentener, F., Muntean, M., Pouliot, G., Keating, T., Zhang, Q., Kurokawa, J., Wankmüller, R., van der Gon, H. D., Klimont, Z., Frost, G., Darras, S., and Koffi, B.: HTAP_v2: a mosaic of regional and global emission gridmaps for 2008 and 2010 to study hemispheric transport of air pollution, Atmospheric Chemistry & Physics Discussions, 15, 12867-12909, 2015.

Jiang, F., Liu, Q., Huang, X., Wang, T., Zhuang, B., and Xie, M.: Regional modeling of secondary organic aerosol over China using WRF/Chem, Journal of Aerosol Science, 43, 57-73, 2012a.

Jiang, F., Zhou, P., Liu, Q., Wang, T., Zhuang, B., and Wang, X.: Modeling tropospheric ozone formation over East China in springtime, Journal of Atmospheric Chemistry, 69, 303-319, 2012b.

Jiang, X., Guenther, A., Potosnak, M., Geron, C., Seco, R., Karl, T., Kim, S., Gu, L., and Pallardy, S.: Isoprene Emission Response to Drought and the Impact on Global Atmospheric Chemistry, Atmos Environ (1994), 183, 69-83, 2018.

Kain, J. S.: The Kain–Fritsch Convective Parameterization: An Update, Journal of Applied Meteorology, 43, 170-181, 2004.

Kim, S.-Y., Jiang, X., Lee, M., Turnipseed, A., Guenther, A., Kim, J.-C., Lee, S.-J., and Kim, S.: Impact of biogenic volatile organic compounds on ozone production at the Taehwa Research Forest near Seoul, South Korea, Atmospheric Environment, 70, 447-453, 2013.

https://doi.org/10.5194/gmd-2021-29
Preprint. Discussion started: 1 March 2021

824 Kok, J. F.: A scaling theory for the size distribution of emitted dust aerosols suggests
825 climate models underestimate the size of the global dust cycle, Proceedings of the
826 National Academy of Sciences, 108, 1016, 2011.
827 Kota, S. H., Schade, G., Estes, M., Boyer, D., and Ying, Q.: Evaluation of MEGAN
828 predicted biogenic isoprene emissions at urban locations in Southeast Texas,
829 Atmospheric Environment, 110, 54-64, 2015.
830 Lehning, A., Zimmer, W., Zimmer, I., and Schnitzler, J. P.: Modeling of annual
831 variations of oak (Quercus robur L.) isoprene synthase activity to predict isoprene
832 emission rates, Journal of Geophysical Research: Atmospheres, 106, 3157-3166,
833 2001.
834 Levis, S., Wiedinmyer, C., Bonan, G. B., and Guenther, A.: Simulating biogenic volatile
835 organic compound emissions in the Community Climate System Model, Journal
836 of Geophysical Research: Atmospheres, 108, 2003.
837 Li, G., Bei, N., Cao, J., Wu, J., Long, X., Feng, T., Dai, W., Liu, S., Zhang, Q., and Tie,
838 X.: Widespread and persistent ozone pollution in eastern China during the non-
839 winter season of 2015: observations and source attributions, Atmos. Chem. Phys.,
840 17, 2759-2774, 2017a.
841 Li, H., Li, L., Huang, C., An, J.-y., Yan, R.-s., Huang, H.-y., Wang, Y.-j., Lu, Q., Wang,
842 Q., Lou, S.-r., Wang, H.-l., Zhou, M., Tao, S.-k., Qiao, L.-p., and Chen, M.-h.:
843 Ozone source apportionment at urban area during a typical photochemical
844 pollution episode in the summer of 2013 in the Yangtze River Delta, Huan jing ke
845 xue= Huanjing kexue, 36, 1-10, 2015a.
846 Li, L., An, J. Y., Zhou, M., Yan, R. S., Huang, C., Lu, Q., Lin, L., Wang, Y. J., Tao, S.
847 K., Qiao, L. P., Zhu, S. H., and Chen, C. H.: Source apportionment of fine particles
848 and its chemical components over the Yangtze River Delta, China during a heavy
849 haze pollution episode, Atmospheric Environment, 123, 415-429, 2015b.
850 Li, L., Yang, W., Xie, S., and Wu, Y.: Estimations and uncertainty of biogenic volatile
851 organic compound emission inventory in China for 2008–2018, Science of The
852 Total Environment, 733, 139301, 2020.
853 Li, L. Y. and Xie, S. D.: Historical variations of biogenic volatile organic compound
854 emission inventories in China, 1981–2003, Atmospheric Environment, 95, 185-
855 196, 2014.
856 Li, M., Liu, H., Geng, G. N., Hong, C. P., Liu, F., Song, Y., Tong, D., Zheng, B., Cui,
857 H. Y., Man, H. Y., Zhang, Q., and He, K. B.: Anthropogenic emission inventories
858 in China: a review, Natl. Sci. Rev., 4, 834-866, 2017b.
859 Li, M., Zhang, Q., Kurokawa, J. I., Woo, J. H., He, K., Lu, Z., Ohara, T., Song, Y.,
860 Streets, D. G., Carmichael, G. R., Cheng, Y., Hong, C., Huo, H., Jiang, X., Kang,
861 S., Liu, F., Su, H., and Zheng, B.: MIX: a mosaic Asian anthropogenic emission
862 inventory under the international collaboration framework of the MICS-Asia and
863 HTAP, Atmos. Chem. Phys., 17, 935-963, 2017c.
864 Liu, Y., Li, L., An, J., Huang, L., Yan, R., Huang, C., Wang, H., Wang, Q., Wang, M.,
865 and Zhang, W.: Estimation of biogenic VOC emissions and its impact on ozone
866 formation over the Yangtze River Delta region, China, Atmospheric Environment,
867 186, 113-128, 2018.

https://doi.org/10.5194/gmd-2021-29
Preprint. Discussion started: 1 March 2021

868 Loveland, T. R., Reed, B. C., Brown, J. F., Ohlen, D. O., Zhu, Z., Yang, L., and
869 Merchant, J. W.: Development of a global land cover characteristics database and
870 IGBP DISCover from 1 km AVHRR data, Int. J. Remote Sens., 21, 1303-1330,
871 2000.
872 Lu, X., Zhang, L., Chen, Y., Zhou, M., Zheng, B., Li, K., Liu, Y., Lin, J., Fu, T. M., and
873 Zhang, Q.: Exploring 2016–2017 surface ozone pollution over China: source
874 contributions and meteorological influences, Atmos. Chem. Phys., 19, 8339-8361,
875 2019.
876 Morrison, H., Thompson, G., and Tatarskii, V.: Impact of Cloud Microphysics on the
877 Development of Trailing Stratiform Precipitation in a Simulated Squall Line:
878 Comparison of One- and Two-Moment Schemes, Monthly Weather Review, 137,
879 991-1007, 2009.
880 Niinemets, Ü., Tenhunen, J. D., Harley, P. C., and Steinbrecher, R.: A model of isoprene
881 emission based on energetic requirements for isoprene synthesis and leaf
882 photosynthetic properties for Liquidambar and Quercus, Plant, Cell &
883 Environment, 22, 1319-1335, 1999.
884 Oleson, K. W., Lawrence, D. M., Bonan, G. B., Flanner, M. G., Kluzek, E., and
885 Lawrence, P. J.: Technical Description of version 4.0 of the Community Land
886 Model (CLM), 2010. 2010.
887 Paulson, C. A.: The mathematical representation of wind speed and temperature profiles
888 in the unstable atmospheric surface layer, J. Appl. Meteorol., 1970. 857-861, 1970.
889 Pierce, T., Geron, C., Bender, L., Dennis, R., Tonnesen, G., and Guenther, A.: Influence
890 of increased isoprene emissions on regional ozone modeling, Journal of
891 Geophysical Research: Atmospheres, 103, 25611-25629, 1998.
892 Poisson, N., Kanakidou, M., and Crutzen, P. J.: Impact of Non-Methane Hydrocarbons
893 on Tropospheric Chemistry and the Oxidizing Power of the Global Troposphere:
894 3-Dimensional Modelling Results, Journal of Atmospheric Chemistry, 36, 157-
895 230, 2000.
896 Safronov, A. N., Shtabkin, Y. A., Berezina, E. V., Skorokhod, A. I., Rakitin, V. S.,
897 Belikov, I. B., and Elansky, N. F.: Isoprene, Methyl Vinyl Ketone and
898 Methacrolein from TROICA-12 Measurements and WRF-CHEM and GEOS-
899 CHEM Simulations in the Far East Region, Atmosphere, 10, 26, 2019.
900 Situ, S., Guenther, A., Wang, X., Jiang, X., Turnipseed, A., Wu, Z., Bai, J., and Wang,
901 X.: Impacts of seasonal and regional variability in biogenic VOC emissions on
902 surface ozone in the Pearl River delta region, China, Atmos. Chem. Phys., 13,
903 11803-11817, 2013.
904 Stauffer, D. R. and Seaman, N. L.: Use of Four-Dimensional Data Assimilation in a
905 Limited-Area Mesoscale Model. Part I: Experiments with Synoptic-Scale Data,
906 Monthly Weather Review, 118, 1250-1277, 1990.
907 Stewart, H. E., Hewitt, C. N., Bunce, R. G. H., Steinbrecher, R., Smiatek, G., and
908 Schoenemeyer, T.: A highly spatially and temporally resolved inventory for
909 biogenic isoprene and monoterpene emissions: Model description and application
910 to Great Britain, Journal of Geophysical Research: Atmospheres, 108, 2003.
911 Thenkabail, P. S., Knox, J. W., Ozdogan, M., Gumma, M. K., Congalton, R. G., Wu, Z.

https://doi.org/10.5194/gmd-2021-29
Preprint. Discussion started: 1 March 2021


Geoscientific Model Development Discussions

912 T., Milesi, C., Finkral, A., Marshall, M., Mariotto, I., You, S. C., Giri, C., and
913 Nagler, P.: ASSESSING FUTURE RISKS TO AGRICULTURAL
914 PRODUCTIVITY, WATER RESOURCES AND FOOD SECURITY: HOW CAN
915 REMOTE SENSING HELP, Photogramm. Eng. Remote Sens., 78, 773-782, 2012.
916 Tie, X., Geng, F., Guenther, A., Cao, J., Greenberg, J., Zhang, R., Apel, E., Li, G.,
917 Weinheimer, A., Chen, J., and Cai, C.: Megacity impacts on regional ozone
918 formation: observations and WRF-Chem modeling for the MIRAGE-Shanghai
919 field campaign, Atmos. Chem. Phys., 13, 5655-5669, 2013.
920 Visser, A. J., Boersma, K. F., Ganzeveld, L. N., and Krol, M. C.: European NOx
921 emissions in WRF-Chem derived from OMI: impacts on summertime surface
922 ozone, Atmos. Chem. Phys., 19, 11821-11841, 2019.
923 Wang, L. H., Follette-Cook, M. B., Newchurch, M. J., Pickering, K. E., Pour-Biazar,
924 A., Kuang, S., Koshak, W., and Peterson, H.: Evaluation of lightning-induced
925 tropospheric ozone enhancements observed by ozone lidar and simulated by
926 WRF/Chem, Atmospheric Environment, 115, 185-191, 2015.
927 Wang, Q. g., Han, Z., Wang, T., and Zhang, R.: Impacts of biogenic emissions of VOC
928 and NOx on tropospheric ozone during summertime in eastern China, Science of
929 The Total Environment, 395, 41-49, 2008.
930 Wang, R., Tie, X., Li, G., Zhao, S., Long, X., Johansson, L., and An, Z.: Effect of ship
931 emissions on O3 in the Yangtze River Delta region of China: Analysis of WRF-
932 Chem modeling, Science of The Total Environment, 683, 360-370, 2019.
933 Wei, W., Lv, Z. F., Li, Y., Wang, L. T., Cheng, S. Y., and Liu, H.: A WRF-Chem model
934 study of the impact of VOCs emission of a huge petrochemical industrial zone on
935 the summertime ozone in Beijing, China, Atmospheric Environment, 175, 44-53,
936 2018.
937 Wei, X. L., Li, Y. S., Lam, K. S., Wang, A. Y., and Wang, T. J.: Impact of biogenic VOC
938 emissions on a tropical cyclone-related ozone episode in the Pearl River Delta
939 region, China, Atmospheric Environment, 41, 7851-7864, 2007.
940 Wiedinmyer, C., Akagi, S. K., Yokelson, R. J., Emmons, L. K., Al-Saadi, J. A., Orlando,
941 J. J., and Soja, A. J.: The Fire INventory from NCAR (FINN): a high resolution
942 global model to estimate the emissions from open burning, Geosci. Model Dev., 4,
943 625-641, 2011.
944 Wild, O., Zhu, X., and Prather, M. J.: Fast-J: Accurate Simulation of In- and Below-
945 Cloud Photolysis in Tropospheric Chemical Models, Journal of Atmospheric
946 Chemistry, 37, 245-282, 2000.
947 Wu, K., Yang, X., Chen, D., Gu, S., Lu, Y., Jiang, Q., Wang, K., Ou, Y., Qian, Y., Shao,
948 P., and Lu, S.: Estimation of biogenic VOC emissions and their corresponding
949 impact on ozone and secondary organic aerosol formation in China, Atmospheric
950 Research, 231, 104656, 2020.
951 Yang, Q., W. I. Gustafson, J., Fast, J. D., Wang, H., Easter, R. C., Morrison, H., Lee, Y.
952 N., Chapman, E. G., Spak, S. N., and Mena-Carrasco, M. A.: Assessing regional
953 scale predictions of aerosols, marine stratocumulus, and their interactions during
954 VOCALS-REx using WRF-Chem, Atmos. Chem. Phys., 11, 11951-11975, 2011.
955 Yarwwod, Wilson.G, Shepaed.S, and Guenther, A.: User's Guide to the Global

https://doi.org/10.5194/gmd-2021-29
Preprint. Discussion started: 1 March 2021

Biosphere Emissions and Interactions System (GloBEIS) Version3, 2002. 2002.

Yin, L., Xu, Z., Liu, M., Xu, T., Wang, T., Liao, W., Li, M., Cai, X., Kang, L., Zhang, H., and Song, Y.: Estimation of biogenic volatile organic compound (BVOC) emissions in China using WRF–CLM–MEGAN coupled model, Biogeosciences Discuss., 2020, 1-30, 2020.

Zaveri, R. A. and Peters, L. K.: A new lumped structure photochemical mechanism for large-scale applications, Journal of Geophysical Research: Atmospheres, 104, 30387-30415, 1999.

Zhang, L., Wang, T., Lv, M., and Zhang, Q.: On the severe haze in Beijing during January 2013: Unraveling the effects of meteorological anomalies with WRF-Chem, Atmospheric Environment, 104, 11-21, 2015.

Zhang, R., Suh, I., Lei, W., Clinkenbeard, A. D., and North, S. W.: Kinetic studies of OH-initiated reactions of isoprene, Journal of Geophysical Research: Atmospheres, 105, 24627-24635, 2000.

Zhao, C., Chen, S., Leung, L. R., Qian, Y., Kok, J. F., Zaveri, R. A., and Huang, J.: Uncertainty in modeling dust mass balance and radiative forcing from size parameterization, Atmos. Chem. Phys., 13, 10733-10753, 2013a.

Zhao, C., Hu, Z., Qian, Y., Ruby Leung, L., Huang, J., Huang, M., Jin, J., Flanner, M. G., Zhang, R., Wang, H., Yan, H., Lu, Z., and Streets, D. G.: Simulating black carbon and dust and their radiative forcing in seasonal snow: a case study over North China with field campaign measurements, Atmos. Chem. Phys., 14, 11475-11491, 2014.

Zhao, C., Huang, M., Fast, J. D., Berg, L. K., Qian, Y., Guenther, A., Gu, D., Shrivastava, M., Liu, Y., Walters, S., Pfister, G., Jin, J., Shilling, J. E., and Warneke, C.: Sensitivity of biogenic volatile organic compounds to land surface parameterizations and vegetation distributions in California, Geoscientific Model Development, 9, 1959-1976, 2016.

Zhao, C., Liu, X., Leung, L. R., Johnson, B., McFarlane, S. A., Gustafson Jr, W. I., Fast, J. D., and Easter, R.: The spatial distribution of mineral dust and its shortwave radiative forcing over North Africa: modeling sensitivities to dust emissions and aerosol size treatments, Atmos. Chem. Phys., 10, 8821-8838, 2010.

Zhao, C., Ruby Leung, L., Easter, R., Hand, J., and Avise, J.: Characterization of speciated aerosol direct radiative forcing over California, Journal of Geophysical Research: Atmospheres, 118, 2372-2388, 2013b.

Zhao, C., Wang, Y., and Zeng, T.: East China Plains: A “Basin” of Ozone Pollution, Environmental Science & Technology, 43, 1911-1915, 2009.

Zheng, J., Zheng, Z., Yu, Y., and Zhong, L.: Temporal, spatial characteristics and uncertainty of biogenic VOC emissions in the Pearl River Delta region, China, Atmospheric Environment, 44, 1960-1969, 2010.

Zhou, G., Xu, J., Xie, Y., Chang, L., Gao, W., Gu, Y., and Zhou, J.: Numerical air quality forecasting over eastern China: An operational application of WRF-Chem, Atmospheric Environment, 153, 94-108, 2017.

Zimmer, W., Steinbrecher, R., Körner, C., and Schnitzler, J. P.: The process-based SIM–BIM model: towards more realistic prediction of isoprene emissions from adult

https://doi.org/10.5194/gmd-2021-29
Preprint. Discussion started: 1 March 2021

Quercus petraea forest trees, Atmospheric Environment, 37, 1665-1671, 2003.

https://doi.org/10.5194/gmd-2021-29
Preprint. Discussion started: 1 March 2021

Geoscientific Model Development Discussions

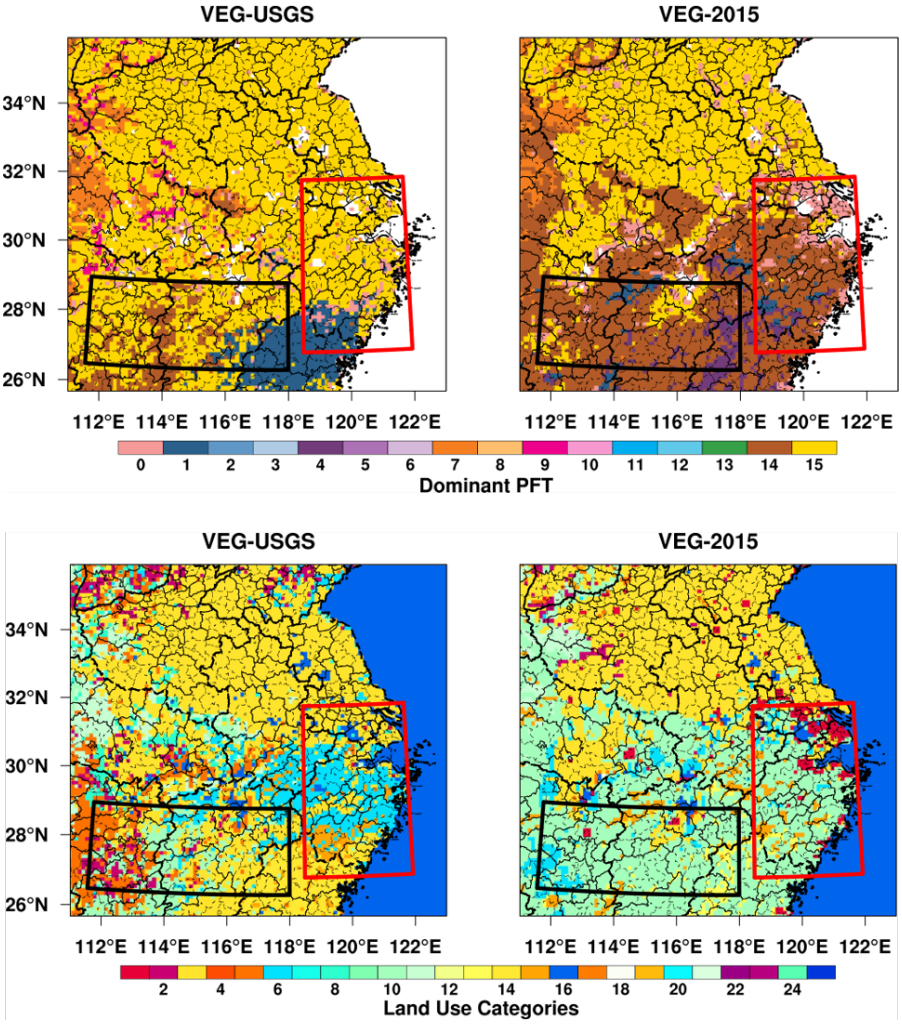

Figure 1. Spatial distribution of two different vegetation data sets (VEG-USGS and VEG-2015) and dominant PFT derived from them in each grid over the simulation domain.

https://doi.org/10.5194/gmd-2021-29
Preprint. Discussion started: 1 March 2021

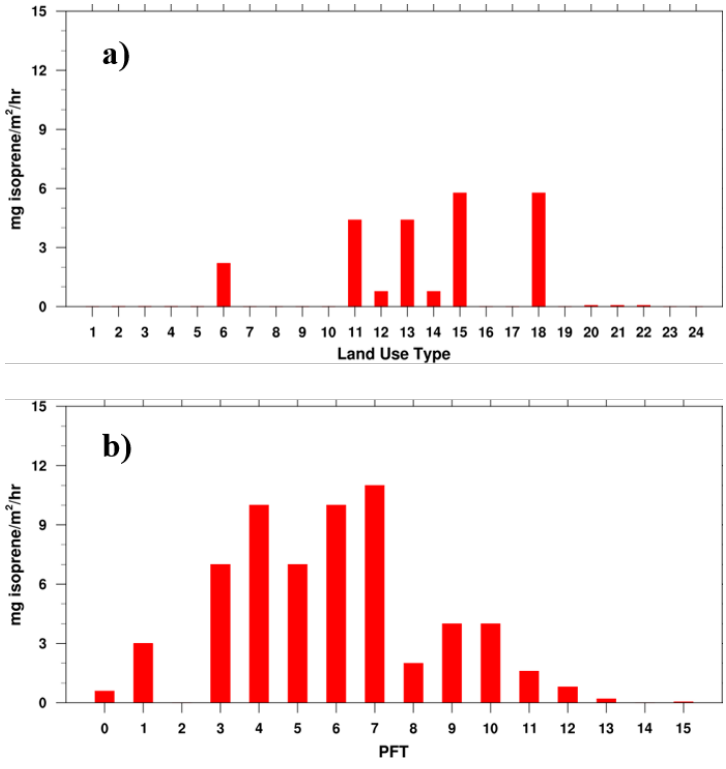

Figure 2. Biogenic emission factor for each land use category in **(a)** MEGAN v1.0, and the land use number 1-24 detailed describe can be found in Table 3 and **(b)** for each PFT in MEGAN v3.0, the PFT number 0-15 are listed in Table 1.

https://doi.org/10.5194/gmd-2021-29
Preprint. Discussion started: 1 March 2021

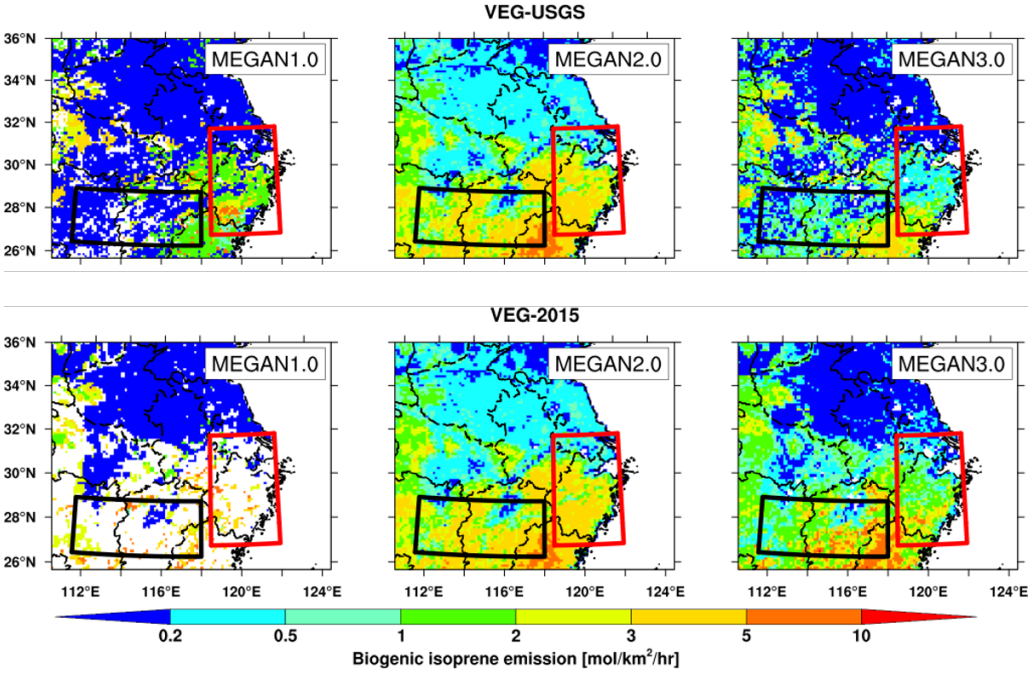

Figure 3. Spatial distributions of biogenic isoprene emissions averaged in April over the simulation domain estimated with different biogenic emission scheme and vegetation data set as listed in Table 1. Two areas are marked by red and black box to discuss the characters in detail.

https://doi.org/10.5194/gmd-2021-29
Preprint. Discussion started: 1 March 2021

Geoscientific Model Development Discussions

1093

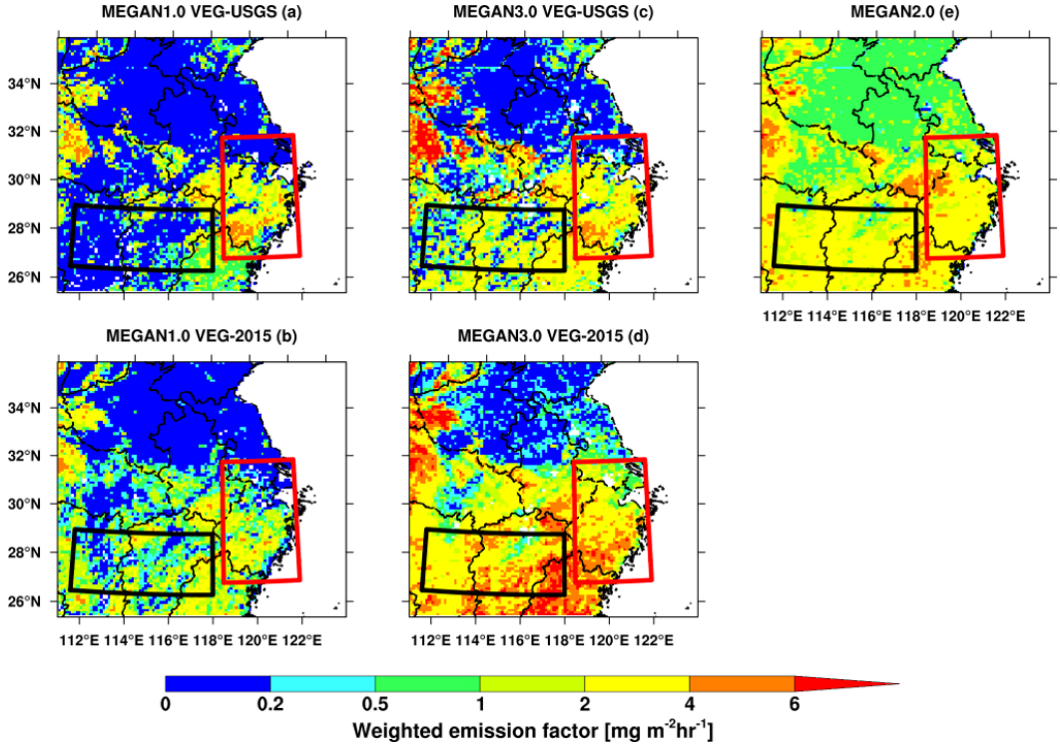

1094

1095 **Figure 4.** Spatial distribution of the weighted mean emission factor derived from
1096 VEG-USGS and VEG-2015 in MEGAN v1.0 **(a)(b)** and MEGAN v3.0 **(c)(d)**.
1097 Meanwhile, **(e)** shows the distribution of isoprene emission factor in MEGAN v2.0
1098 database.

1099

1100

1101

1102

1103

1104

1105

1106

1107

https://doi.org/10.5194/gmd-2021-29
Preprint. Discussion started: 1 March 2021

Geoscientific Model Development Discussions
Open Access
EGU

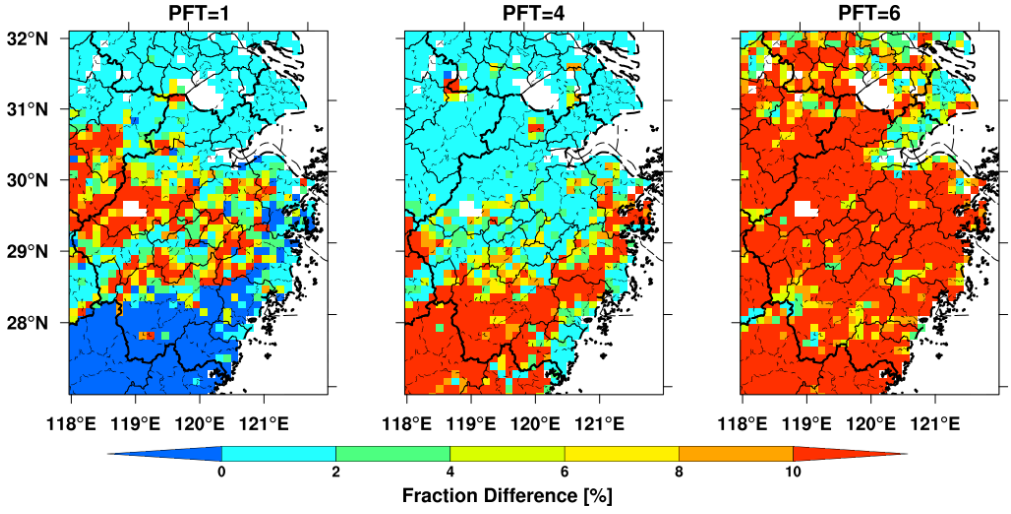

Figure 5. Spatial distribution of the PFT percentage difference between the VEG-2015 and VEG-USGS (VEG-2015 minus VEG-USGS) for needle-leaf evergreen tree, broadleaf evergreen tree and broadleaf deciduous tree.

https://doi.org/10.5194/gmd-2021-29
Preprint. Discussion started: 1 March 2021

Geoscientific Model Development Discussions

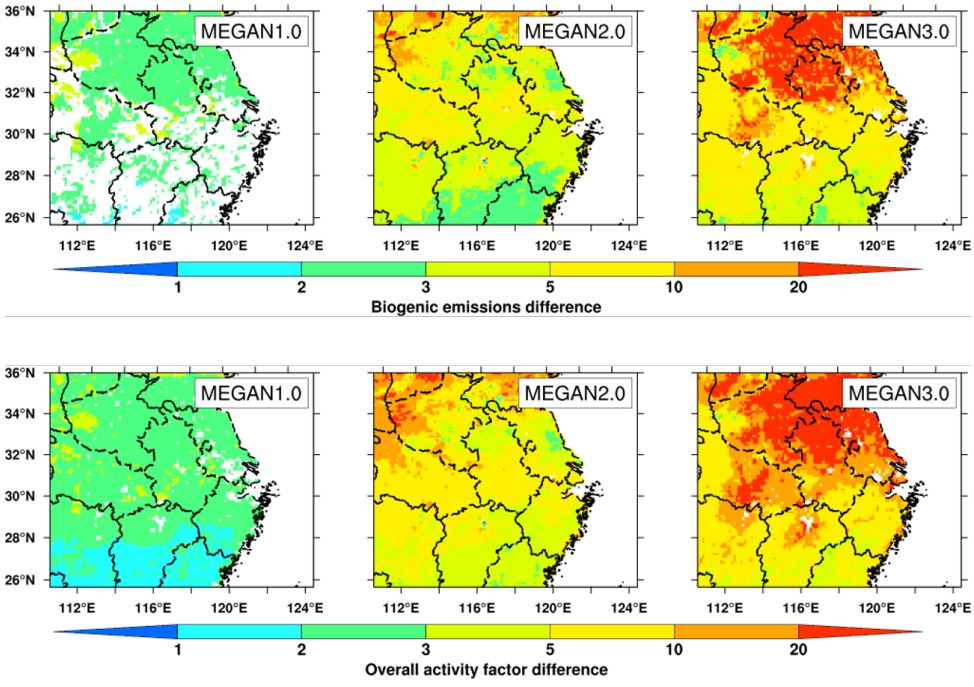

Figure 6. Spatial distribution of the quotient of biogenic isoprene emission and activity factor between simulations using VEG-2015 vegetation data set in July and that in April.

https://doi.org/10.5194/gmd-2021-29
Preprint. Discussion started: 1 March 2021

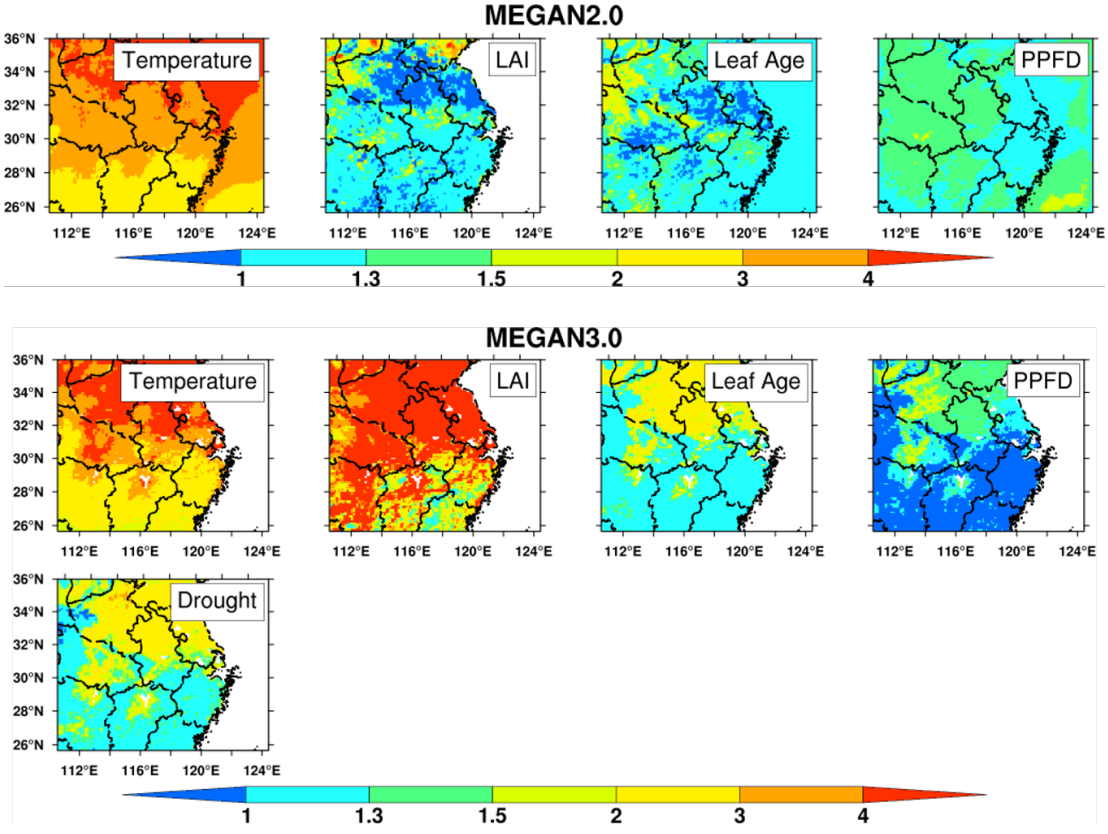

Figure 7. Spatial distribution of the quotient of activity factor related to different environmental variables (such as temperature, LAI, light, leaf age and drought) between simulations in July and that in April (July divided by April) using VEG-2015 vegetation data set coupled with MEGAN v2.0 and MEGAN v3.0.

https://doi.org/10.5194/gmd-2021-29
Preprint. Discussion started: 1 March 2021

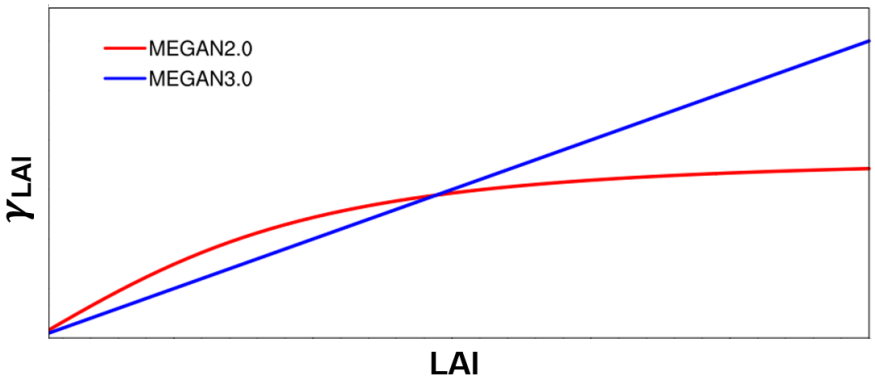

Figure 8. Activity factor for LAI (γ_{LAI}) variation with LAI in different versions of MEGAN, red line represent the MEGAN v2.0 and blue line for MEGAN v3.0

https://doi.org/10.5194/gmd-2021-29
Preprint. Discussion started: 1 March 2021

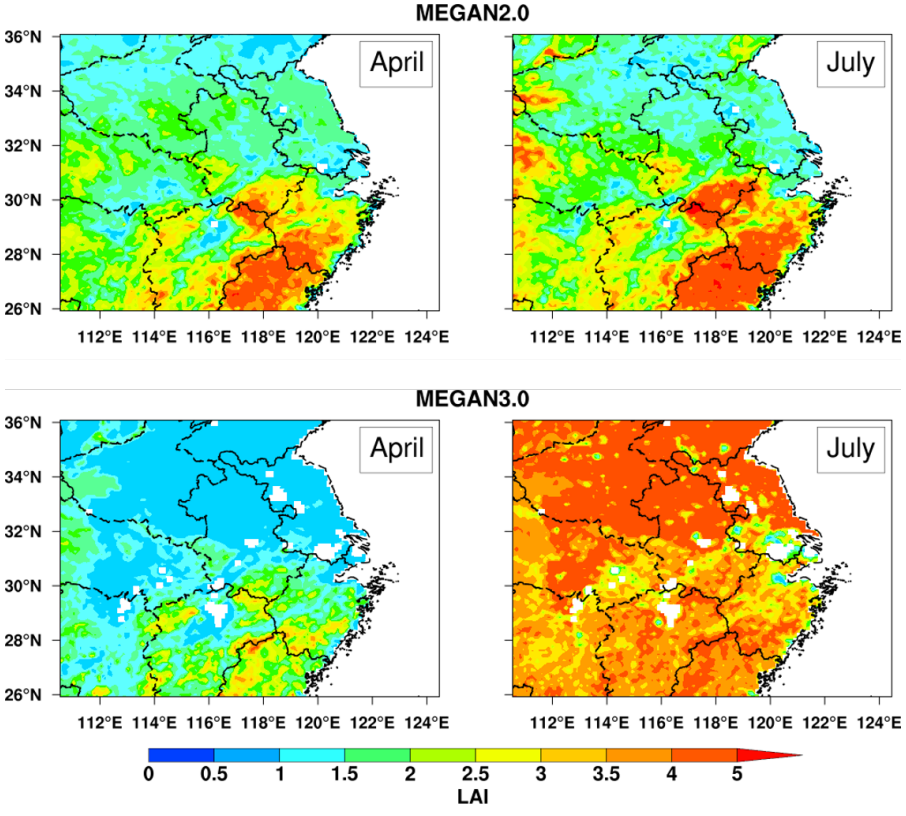

Figure 9. The spatial distribution of monthly leaf area index (LAI) from VEG-2015 in the MEGAN v2.0 and MEGAN v3.0.

https://doi.org/10.5194/gmd-2021-29
Preprint. Discussion started: 1 March 2021

Geoscientific Model Development Discussions

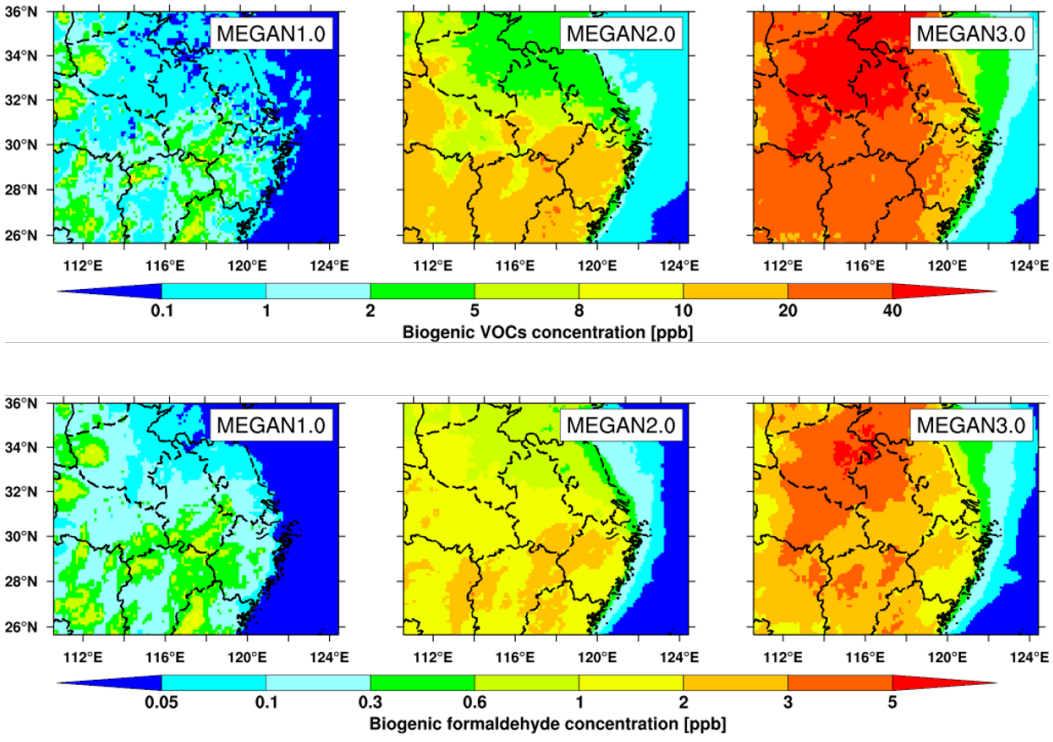

Figure 10. Spatial distribution of VOCs and formaldehyde concentration due to the biogenic emissions (minus anthropogenic emissions) near the surface in July using the VEG-2015 vegetation date set.

https://doi.org/10.5194/gmd-2021-29
Preprint. Discussion started: 1 March 2021

Geoscientific Model Development Discussions

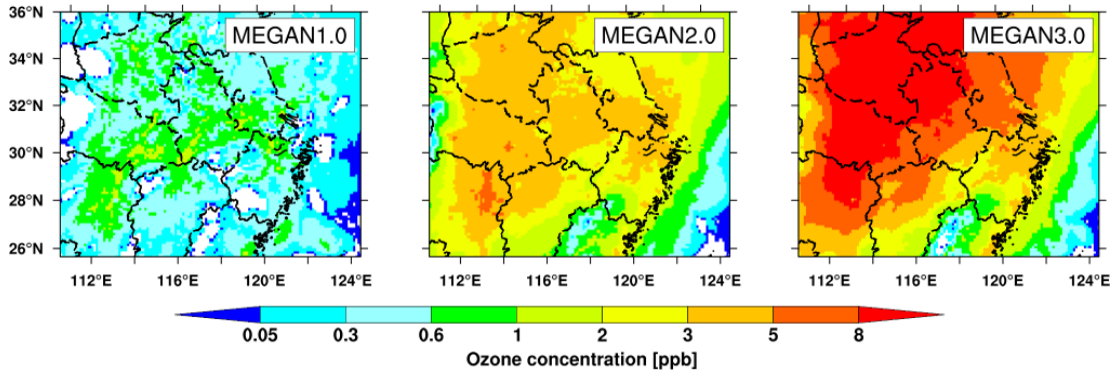

Figure 11. Spatial distribution of ozone concentration due to the biogenic emissions near the surface in July using the VEG-2015 vegetation date set.

https://doi.org/10.5194/gmd-2021-29
Preprint. Discussion started: 1 March 2021

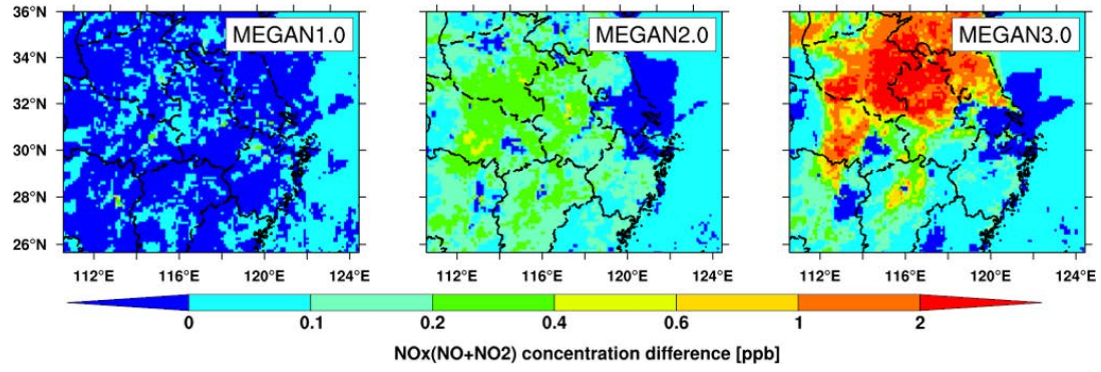

Figure 12. Spatial distribution of NOx concentration due to the biogenic emissions near the surface (the difference of simulation considered biogenic emissions and the one without biogenic emissions) in July using the VEG-2015 vegetation date set.

https://doi.org/10.5194/gmd-2021-29
Preprint. Discussion started: 1 March 2021

Geoscientific Model Development Discussions

Table 1 The domain averaged fraction of PFTs in two vegetation data sets

PFT number	description	VEG-USGS	VEG-2015
0	Bare soil	3.7	6.9
1	Needleleaf evergreen tree–temperature	7.9	1.7
2	Needleleaf evergreen tree–boreal	0	0
3	Needleleaf deciduous tree–boreal	0	0
4	Broadleaf evergreen tree–tropical	0	4.5
5	Broadleaf evergreen tree–temperature	0	0
6	Broadleaf deciduous tree–tropical	0	0
7	Broadleaf deciduous tree–temperature	7.6	4.4
8	Broadleaf deciduous tree–boreal	0	0
9	Broadleaf evergreen shrub–temperature	1.8	0
10	Broadleaf deciduous shrub–temperature	0	0
11	Broadleaf deciduous shrub–boreal	0	0
12	C_3 arctic grass	0	0
13	C_3 grass	0	0
14	C_4 grass	8.7	41.6
15	Crop	70.2	40.8

https://doi.org/10.5194/gmd-2021-29
Preprint. Discussion started: 1 March 2021

Geoscientific Model Development Discussions

Table 2 Numerical experiments of WRF-Chem in this study.

	Simulation period	BVOC scheme	Vegetation distribution	
			VEG-USGS	VEG-2015
WRF-Chem	April	MEGAN v1.0	Mv1-USGS	Mv1-2015/Mv1-April
		MEGAN v2.0	Mv2-USGS	Mv2-2015/Mv2-April
		MEGAN v3.0	Mv3-USGS	Mv3-2015/Mv3-April
	July	MEGAN v1.0	-	Mv1-July
		MEGAN v2.0	-	Mv2-July
		MEGAN v3.0	-	Mv3-July

https://doi.org/10.5194/gmd-2021-29
Preprint. Discussion started: 1 March 2021

Geoscientific Model Development Discussions

Table 3 Measured and simulated isoprene concentrations (ppbv) at sampling sites.

Location	Observation	Simulation			Source
		MEGANv1.0	MEGANv2.0	MEGANv3.0	
Lishui District, Nanjing	0.062	0.010	0.071	0.049	observation
Xujiahui commercial center, Shanghai	0.120	0.020	0.075	0.090	Cai et al. (2010)
Northern suburb, Nanjing	0.960±0.56	0.017	0.905	0.073	Shao et al. (2016)
Nanjing University of Information Science&Technology	0.300±0.35	0.023	0.171	0.180	Li et al. (2014)
Hubei Provincial Environmental Monitoring Center, Wuhan	0.380(0.18-0.6)	0.130	0.997	1.090	Lyu et al. (2016)